

USE OF FLOODPLAIN DENDROCHRONOLOGY IN CAT ISLAND NATIONAL  
WILDLIFE REFUGE TO EXAMINE MISSISSIPPI RIVER FLOOD HISTORY

A THESIS

SUBMITTED ON THE SIXTH DAY OF FEBRUARY 2024

THE DEPARTMENT OF EARTH AND ENVIRONMENTAL SCIENCES

IN PARTIAL FULFILMENT OF THE REQUIREMENTS

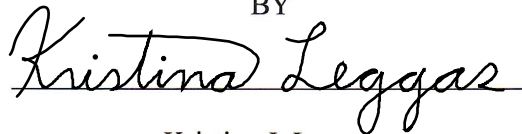
OF THE SCHOOL OF SCIENCE AND ENGINEERING

FOR THE DEGREE

OF

MASTER OF SCIENCE

BY

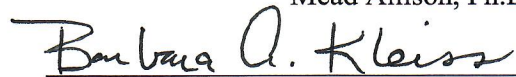


Kristina J. Leggas

APPROVED:

**Mead Allison** Digitally signed by Mead Allison  
Date: 2024.02.07 11:21:41 -06'00'

Mead Allison, Ph.D.



Barbara A. Kleiss, Ph.D.

BEANE.NATHAN.R.1400 Digitally signed by  
942800 BEANE.NATHAN.R.1400942800  
Date: 2024.02.07 07:16:46 -06'00'

Nathan Beane, Ph.D.



Nicole Gasparini, Ph.D.



## ACKNOWLEDGMENTS

Funding for this study was provided by the Science and Technology Office, US Army Corps of Engineers Mississippi Valley Division. Thank you to the Cat Island refuge manager, Jimmy Laurent, for assistance with access to the park. Thank you to all of those who helped core and sand all the cypress cores —Dr. Nathan Beane and his team at ERDC, especially Matt Blanchard— and to Dr. Barb Kleiss and Dr. Mead Allison for digging up many feldspar plots and helping me find all the water loggers. Thank you to Dr. Colin Jackson and his students for letting me use their lab space, microscope and camera. Thank you to Dr. Clay Tucker for all of his much-needed expertise on baldcypress trees and dendrochronology. Last but not least, thank you to my committee members Dr. Mead Allison, Dr. Barb Kleiss, Dr. Nathan Beane and Dr. Nicole Gasparini for all your advice, help and getting me to the finish line.

## TABLE OF CONTENTS

ACKNOWLEDGEMENTS.....	i
List of Tables .....	iv
List of Figures.....	v
1. INTRODUCTION.....	1
2. BACKGROUND.....	5
2.1 Dendrochronology in Baldcypress .....	6
2.2 Applications of Dendrochronology .....	10
2.3 Engineering and Flooding History of the Lower Mississippi River Basin .....	12
3. CAT ISLAND STUDY AREA .....	18
4. METHODS.....	24
4.1 Tree Coring .....	24
4.2 Tree Core Preparation and Analysis .....	27
4.3 Water Level Loggers .....	28
4.4 Feldspar Plots .....	29
4.5 Analysis of Mississippi River Historic Stage and Discharge Records .....	29
5. RESULTS .....	33
5.1 Dendrochronology .....	33
5.2 Floodplain Inundation at Cat Island in WY 2022 .....	36

Mississippi River Historical Stage and Discharge .....	39
5.4 Feldspar Plot Sediment Deposition in WY 2022 .....	45
6. DISCUSSION.....	48
6.1 Correlation with Individual Baldcypress Site Elevation .....	48
6.2 Baldcypress Chronology Correlation to Local Climatology .....	51
6.3 Baldcypress Chronology Correlation to Regional Climate Trends .....	51
6.4 Baldcypress Chronology Correlation to Mississippi River Historic Record.....	57
6.4.1 Correlation with Duration of Inundation .....	60
6.4.2 Correlation with Maximum Stage .....	62
6.4.3 Correlation with Discharge .....	65
6.5 Relationship to Mississippi River Historic Engineering .....	67
6.6 Future Considerations for Utilizing Baldcypress Chronologies .....	71
7. CONCLUSIONS .....	74
APPENDICES .....	76
Appendix A: Baldcypress Chronology Information.....	76
Appendix B: Deposition field measurements.....	80
Appendix C: Individual Baldcypress Correlations.....	84
REFERENCES .....	86

## List of Tables

**Table 1.** Data compiled for MR hydrologic records in proximity to the study area.

**Table 2.** Descriptive statistics from COFECHA program output.

**Table 3.** HOBO water level logger gage information for the WY2022 experiment.

**Table 4.** Elevation and river inundation statistics for sample sites in Cat Island where both a HOBO water level record and tree cores were collected.

**Table 5.** Pearson product-moment correlations of local climatological records (New Roads, LA) to ring width index (RWI).

**Table 6:** Pearson product-moment correlation coefficients for RWI and long-term LMR hydrologic data with their period of record.

## List of Figures

**Figure 1.** Annual growth rings in baldcypress.

**Figure 2.** False rings shown in two baldcypress sample cores.

**Figure 3.** LMR from ORCC to Baton Rouge including the location of the CIWR, water and flood control structures and the location of stage and discharge gages.

**Figure 4.** Migration of the Mississippi River channel since 1765 adjacent to the CIWR meander bend.

**Figure 5.** Daily MR Stage (NWIS) at Baton Rouge, LA.

**Figure 6.** (A) Length of inundation for WY 2021 in days for the CIWR meander bend floodplain area. (B) Elevation data CIWR from The Louisiana Statewide GIS obtained by airborne LiDAR.

**Figure 7.** Predominant landcover types in the CIWR area which is the highlighted area in red on the left descending bank of the MR.

**Figure 8.** Field sample locations at Cat Island NWR for baldcypress tree cores, feldspar plots and HOBO water level loggers.

**Figure 9.** Tree coring on a ladder at CIWR to sample above the buttress.

**Figure 10.** Ring width index for the final master chronology.

**Figure 15.** Daily stage records for stations in proximity to the study area.

**Figure 16.** Peak stage seasonality at CIWR derived from daily stage elevation.

**Figure 17.** Days of inundation per year at CIWR derived from daily stage data.

**Figure 18.** Yearly peak stage for gages near study area.

**Figure 19.** Yearly average Mississippi River water discharge at Baton Rouge, LA and Tarbert Landing, MS.

**Figure 20.** Comparison of days inundated at CIWR in WY 2021 and WY 2022

**Figure 21.** Feldspar deposition measurements for WY 2020-2022

**Figure 22.** Example of the individual tree growth and calculated duration of inundation at Site TADI29

**Figure 23.** Maximum temperature Pearson's correlation to RWI by season

**Figure 24.** PDSI averaged over 1-year Pearson's correlation to RWI.

**Figure 25.** PDSI averaged over 3-month periods Pearson's correlation to RWI.

**Figure 26.** (A) Duration of inundation at CIWR based on gage height readings compared to RWI. (B) Best fit linear regression (red line) between these criteria.

**Figure 27.** Maximum stage record at Red River Landing, LA compared to RWI record (A). Linear relationship between both records (B).

**Figure 28.** Relationship between duration of inundation and yearly maximum stage showing increased duration with increased maximum stage.

**Figure 29.** Specific gage record at Red River Landing, LA

**Figure 30.** Correlation of baldcypress RWI index to month of maximum stage.

**Figure 31.** Condensed timeline of engineering on the lowermost MR

**Figure 32.** Difference in water at Vicksburg and Tarbert Landing



## 1. INTRODUCTION

Dendrochronology is the study of annual tree growth rings. The origins of the word are from the Greek language: *dendro* meaning tree, *chronos* meaning time, and *ology* meaning the study of. Dendrochronology has been utilized as a proxy for many environmental variables, including pollution, precipitation and insect outbreaks (Speer, 2012). Flooding, drought and climate change may also be recorded in tree ring records. Width of tree rings, used as the proxy, are denoted by changes in the cell walls to differentiate years of growth in a tree (Frank et al., 2022). Increases or decreases in annual tree growth increments can be indicative of the aforementioned changes in environmental factors.

The use of dendrochronology in riparian settings has previously been utilized to provide insights into historical flooding events and the past hydrology of an area. Baldcypress (*Taxodium distichum*; USDA, 2024) within riparian forests of the southeastern United States have been shown to be responsive to hydrologic changes in adjacent rivers (Therrell et al., 2020), with radial growth of trees correlated to the availability of water during the growing season (Keim and Amos, 2012). Using dendrochronological techniques, the present study examines baldcypress in riparian systems at Cat Island National Wildlife Refuge (NWR) along the Lower Mississippi River (LMR, defined as the reach below the confluence of the Ohio River to the Gulf of Mexico). The present study seeks to examine the historical record of the connection between the floodplain and the LMR channel as recorded by baldcypress tree ring records. Cat Island NWR is one of the largest areas of floodplain in the LMR that remains in hydrologic connection with the channel due to the absence of artificial levees

in this reach of the river. Specifically, this research will determine if baldcypress trees in Cat Island contain a dendrochronological record of annual flood magnitude and/or duration that can potentially document hydrological changes wrought by human engineering, as well as can potentially extend the LMR hydrologic period of flood record at Cat Island and elsewhere in the LMR to before instrumented flood monitoring began ~150 y ago.

The LMR has been heavily engineered for over a century, primarily to improve navigability and reduce flood risks to communities along its course. Levees, dams, cutoffs, dikes and revetments have significantly altered the course and hydrology of the LMR and the entire Mississippi River system (Alexander et al., 2012). These alterations to the river have heavily restricted the hydrologic connectivity between the main channel and the floodplain, as well as in many areas, simplified the channel, altered sediment magnitude and timing, and lowered river channel bed elevation. Consequently, processes that normally connect the river channel and the floodplain, such as channel migration and overbanking during floods, are restricted by revetments and levees in much of the LMR (Allison et al., 2012; Murray and Biedenharn, 2022). Channel connection to the floodplain has been eliminated along much of the Mississippi River above and below the confluence with the Ohio, except during extremely high flow or levee failure events (Alexander et al., 2012). Peak discharge has significantly decreased and low discharge has increased, specifically downstream of dams, and the seasonality of discharge has also been altered due to the effect of reservoir dams in major tributaries (e.g., Missouri and Arkansas Rivers). Further, engineering efforts in the Mississippi catchment are estimated

to have decreased the area of floodplain inundation by 90 percent (Alexander et al., 2012).

This disruption in channel connectivity to the floodplain alters water, sediment and nutrient supply to these floodplain environments (Allison et al., 2012). These resources ensure normal wetland ecosystem functions occur, as well as assisting with successful regeneration of floodplain forests (Meitzen, 2018). The floodplain of the LMR is a highly dynamic environment, providing many valuable ecosystem services and habitats for a diverse community of organisms (Biedenharn et al., 2018). The connectivity of the river to the floodplain allows for changes in riverine hydrology to alter the floodplain, affecting its vegetation, sedimentation and hydrology through seasonal and annual inundation. Understanding the floodplain forest's response to alterations in the LMR is critical to management decisions. This response will be examined in the present study through tree growth and their response to yearly hydrological changes.

The main objective of this study is to utilize dendrological techniques to create and analyze a chronology of baldcypress growth patterns in Cat Island NWR to gain a better understanding of the floodplain's response to engineering and land use changes in the LMR since Western colonization. The initial goal is to determine if tree ring records from Cat Island NWR that remain in hydrologic connection to the channel preserve a record of annual flood magnitude and/or duration in the LMR. The potential significance of this would be (1) to provide a record of flooding within CIWR and the extent to which that overbanking record has been impacted by anthropogenic alterations to the catchment, and (2) develop a methodology that ultimately will allow for a reconstruction of flood history that exceeds the ~150-year instrument record of LMR discharge. The first would

be of value to give insight into how engineering changes to the channel have affected the floodplain forest and latter would be of value in lengthening the period of record for determining whether climate change is impacting Mississippi discharge at present and into the future. This chronology, used to evaluate annual tree growth, will show ring width indices, an index of radial tree growth by year (Xu, 2017). The tree ring data will be compared to the LMR hydrographic record to determine correlations between annual growth and stage. Further, the baldcypress chronology will be compared to the LMR historical hydrographic record (e.g., river stage or discharge) to examine what aspects of flooding the tree ring record is sensitive to, including seasonality, duration, or magnitude of Water Year (WY, defined as October 1- September 30) time series. Flood records of inundation depth and timing obtained from within Cat Island NWR in WY 2021-2022 as part of the present study will be utilized to examine how river stage relates to flood depth at various elevations and localities within the floodplain. The relationship between tree cores and their growth rate as related to river stage will be used to determine the extent to which baldcypress trees contain a record of the river's present and historical annual hydrological cycle.

## 2. BACKGROUND

Baldcypress are found throughout the southeastern United States, distributed from Texas along the Gulf Coast to Florida, up the eastern coast to Virginia, and are found in the Mississippi basin from Louisiana to Illinois (Wilhite & Toliver, 1990). Throughout the Southeast, baldcypress are found in four distinct environments: alluvial swamps along rivers and streams with abundant sediments (such as the Mississippi River), spring and seepage sourced non-alluvial streams, slightly brackish swamps in proximity to the coast and upland nutrient-deprived ponds (Stahle et al., 2012). The present study takes place in the first listed habitat, which may be ideal conditions for the species to dominate due to their regeneration methods and ability to thrive in wet conditions. While established trees can continue to grow if flooded during the growing season, seedlings can only survive submersion in the dormant season and need ample time to grow before being inundated during the growing season to survive –at least to the extent to where their foliage is not entirely submerged (Keeland and Conner, 1999). Hence, annual recruitment is closely linked to the magnitude and timing of riverine flooding in environments such as the present study area. The episodic nature of overbank flood peaks in a WY in the LMR, and the occurrence of low flood years, allows for dry periods of varying length from year-to-year during the growing season. However, flooding can be beneficial as baldcypress use floodwaters to disperse the seeds that they drop during the fall/winter season (Meitzen, 2018). Once seeds are dispersed, sufficient soil moisture and sunlight is needed for seedlings to germinate and establish (Keeland and Conner, 1999). Baldcypress often occur in swales of the floodplain (Meitzen, 2018) including those at Cat Island, which can provide moist soil conditions even during periods when the floodplain is not

inundated. Whether the seedlings that germinate during a given dry interval survive to maturity will be determined by the depth and timing of inundation during subsequent WY until the trees reach sufficient height to remain emergent throughout the year.

### ***2.1 Dendrochronology in Baldcypress Trees***

In the science of dendrochronology, annual ring widths (Figure 1) and false rings (Figure 2) in baldcypress trees have been shown to record hydrologic and climatic events (Kiem and Amos, 2012; Stahle et al., 2012; Therrell et al., 2020; Tucker et al., 2022). Both types of ring formation are determined by the presence of earlywood and latewood. Earlywood occurs at the beginning of the growing season (i.e., Spring) and is characterized by larger cells with thin cell walls, whereas latewood occurs once tree growth slows (i.e., Autumn) and is characterized by smaller cells with thicker cell walls. Annual tree ring width (hereafter ring width) is defined as the distance between the end of one latewood band to the end of the next. False rings may also appear in baldcypress when water availability increases once the growing season has begun (Tucker et al., 2022). This water increase allows for more rapid tree growth after initial growth has slowed and the latewood has already begun to form. This pattern is observed when a gradual decrease is immediately followed by a gradual increase in cell size within an annual ring but imitates the appearance of an annual ring—hence a false ring assignment. Baldcypress growth in the floodplain typically has a positive response to inundation, beginning as water enters the floodplains and slowing as it recedes (Stahle et al., 2012). The ability to increase growth during longer periods of inundation is exceptional to baldcypress as other species' growth will typically stop if flooded for the duration of those at Cat Island NWR (Kiem and Amos, 2012; Stahle et al., 2012; Tucker et al., 2022).

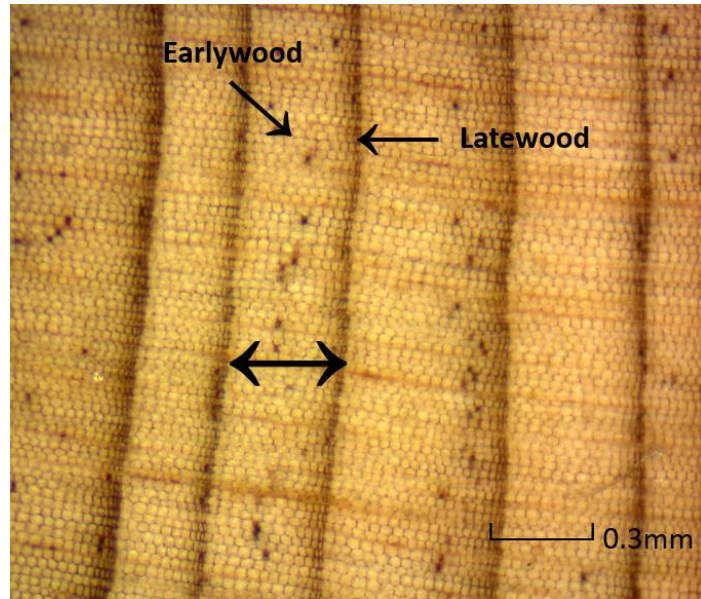


**Figure 1:** Photomicrograph of annual growth rings in baldcypress from an individual tree core sample in the present study. One year of growth and annual ring width is denoted by the double-headed arrows.

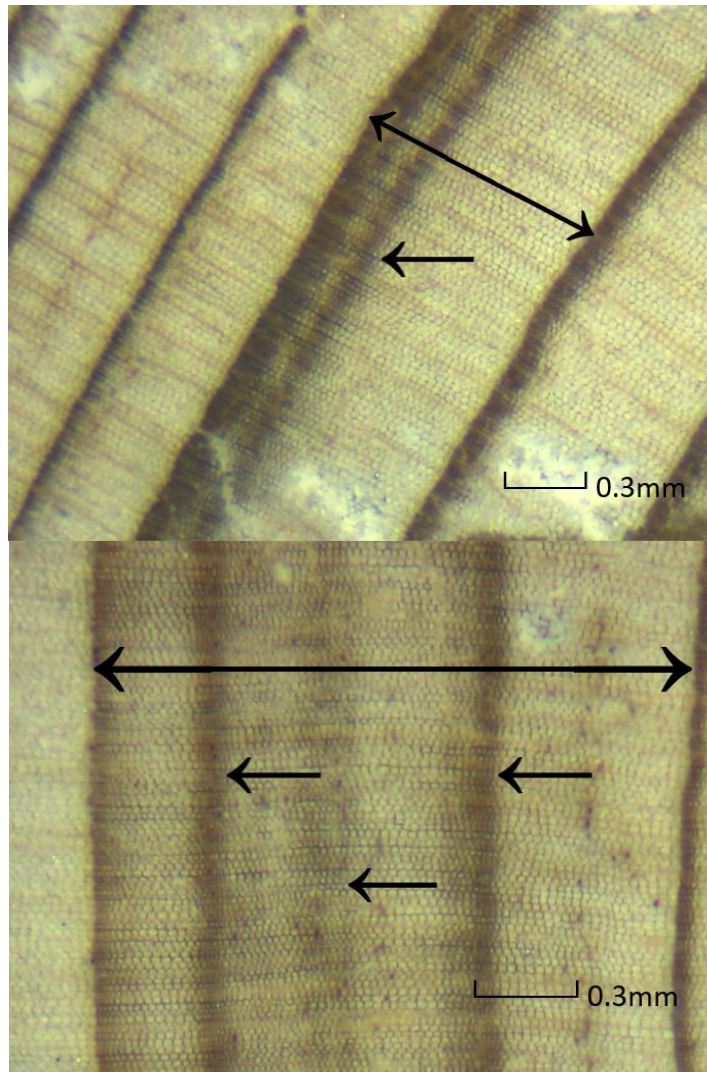


**Figure 2:** Photomicrograph of false rings (denoted by single-headed arrows) in two baldcypress sample cores from the present study. Annual rings are denoted by double-headed arrow.

Previous studies have successfully used false rings as a proxy for understanding past hydroclimatic events (Kiem and Amos, 2012; Therrell et al., 2020; Tucker et al., 2022). The occurrence of false rings in a given year's growth may be representative of events such as rainfall associated with hurricanes, or abruptly spiked streamflow and re-inundation of the floodplain. Analysis of total ring width has been shown to preserve a record of interannual variations in streamflow (Kiem and Amos, 2012). Further,

variations within ring width indices of chronologies have illustrated hydrologic history, with increases in yearly inundation positively correlated to yearly growth (Kiem and Amos, 2012). Initial studies of ring width chronologies in baldcypress have been shown to be a valuable tool for obtaining a long-term record in hydrologic history (Kiem and Amos, 2012; Therrell et al., 2020; Tucker et al., 2022). The present study attempts to compare chronology correlation to multiple characteristics of yearly inundation—magnitude, duration and seasonality, to determine which correlation may be most useful in examining long-term hydrologic records. Further the study examines how baldcypress chronologies may be used to observe hydrologic changes wrought by human engineering on the LMR that have resulted in variations in stage magnitude and timing.

In the field of dendrochronology, crossdating is a fundamental method that allows for the verification of annual dates of tree cores. Crossdating is performed by matching dates on annual rings between cores taken from multiple trees in the same setting (e.g., within a connected forested area with similar management or disturbance history). This method of cross-matching ring patterns is possible because of the variation in limiting environmental factors impacting growth of multiple trees, and hence, variation in tree growth year-by-year can be associated with changes in overarching environmental factors such as rainfall or degree and timing of flooding. The appearance of ring width variation must be replicated throughout the samples of cores from multiple trees to validate yearly rings (Speer, 2012). A master chronology incorporating multiple tree cores can be built once all tree cores are cross dated. A chronology is built of multiple tree core series. The term “Series” typically denotes the measurements of ring width taken from one tree core.

Baldcypress is considered a sensitive tree to variations in environmental conditions, displaying a high variability in yearly growth. *Sensitive* trees are referred to as trees with ring widths that vary significantly from year to year and *complacent* trees are species that have similar ring widths from year to year (Speer, 2012). The variation of growth in baldcypress is useful in crossdating, however, the frequent occurrence of false rings in baldcypress tree cores complicates successful crossdating. Additionally, baldcypress characteristically possesses numerous false rings. False rings may appear as annual rings and annual rings may appear as false rings. Additionally, rings may appear as false in one radial segment of a ring and annual in another segment. Overall, however, the sensitivity of baldcypress growth to hydrologic changes and the seasonality of inundation in a study area, makes their tree rings a viable proxy for inundation. This sensitivity, by resulting in high variability in the ring widths, increases ability to crossdate samples while simultaneously contributing to difficulties in verifying annual ring ages.

## ***2.2 Applications of Dendrochronology***

Dendrochronology has a wide range of applications, including the detection of patterns that correlate to environmental conditions (Speer, 2012). Specifically, dendrochronology may be useful in studying past hydrology as a limitation of studying long-term flood regime records is the absence of long-term water monitoring of a river basin. Multiple studies have provided a record of long-term and paleo hydrology using tree ring records (Therrell and Bialecki, 2015; Keim and Amos, 2012; Meko and Therrell, 2020; Tucker et al., 2022) suggesting that dendrochronology can be used to improve our understanding of river catchment hydrology where baldcypress are found. Further applications include the examination of tree rings to study various geomorphological

systems (Stoffel and Bollschweiler, 2008). Therrell and Bialecki (2015) state that physical damage to trees wrought by flooding can be examined to indicate inundation history. This is referring to damage to the cells during the growing period, which is then recorded in the annual growth ring. Their study used flood rings in overcup oak (*Quercus lyrata*; USDA, 2024) 60 kilometers downstream of the confluence of the Mississippi and Ohio Rivers to construct records of major flooding events, particularly in the spring season, recording these events with the occurrence of a flood ring in nearly all spring floods over the analyzed period of dendrochronological record (1770-2009). Meko and Therrell (2020) utilized flood rings in overcup oak to build a flood chronology spanning the years 1780-2013 at the confluence of the White and Mississippi Rivers. They also utilized earlywood vessel width measurements to reconstruct spring river levels from the years 1800-2013. Keim and Amos (2012) compared hydrologic records over 51 year period to a 111 year record in baldcypress using tree ring chronologies from multiple swamps in the Mississippi Delta and found that the baldcypress chronologies are a better record of hydrology –depth and duration of inundation– than climatology (e.g., rainfall or temperature) in the study area. A drawback of typical dendrochronology records for reconstructing hydrology is that trees are typically more sensitive to drought than flood conditions. As baldcypress are one of the most sensitive trees to flood conditions positively impacting their annual growth rates (Kiem and Amos, 2012; Tucker et al., 2022), it is anticipated they will allow for the examination duration, seasonality and magnitude of inundation in the present study area. Existing studies have not correlated baldcypress tree ring width variability to parameters of inundation in the multi-faceted manner of the present study. Specifically, duration is not often studied throughout the

literature, and water discharge is typically the sole parameter used to correlate baldcypress chronologies to their adjacent rivers.

### ***2.3 Engineering and Flooding History of the Lower Mississippi River Basin***

The LMR has a complex history of engineering alterations beginning in the late 1800s and 1900s. These alterations have been linked to the historical pattern of land-use change in the Mississippi catchment with western colonization beginning in the second half of the 18<sup>th</sup> century (Cole et al., 1998; Billington et al., 2001; Steyaert and Knox, 2008; Li et al., 2022). Collectively, these activities have strongly impacted (1) the areal extent of the floodplain remaining in hydrologic connection with the channel, and (2) water volume and sediment load passing the present Cat Island NWR study area.

The Flood Control Act of 1917 was the first instance of larger-scale construction works coordinated by the federal government on the LMR in the 1900s. It resulted in the construction of weak, unregulated levees and began isolation of the floodplain from the channel (Mississippi River Commission, 2007). The Great Flood of 1927 caused widespread devastation and prompted a federal effort to improve means at which to manage the river to reduce flooding impacts through the Mississippi River and Tributaries (MR&T) Act of 1930. The MR&T program raised and improved the LMR levee system to a federal standard and constructed a series of spillways in the lowermost section in Louisiana to divert water out of the channel in extreme events such as the 1927 flood (Alexander et al., 2012). The MR&T program's engineering heavily constrained channel migration in the final reach from Baton Rouge, LA to the Gulf of Mexico.

Additionally, this further isolated the floodplain in most of the LMR from receiving overbank flows during floods.

Annual seasonal floods throughout the LMR typically caused overbank inundation of the floodplain along the channel prior to the levee system. After MR&T levee construction, most of the floodplain is isolated and does not receive annual supply of water and sediment from the river, except in cases of levee failure. Further, the constriction of the channel increased channel flow. Spillway construction included the Bonnet Carré Spillway (Figure 3), immediately upriver from New Orleans, LA in 1929-1931, that was designed to divert a maximum of 250,000 cfs (7,079 cms) to keep discharge at New Orleans below a maximum of 1,250,000 cfs (~35,000 cms; Lewis et al., 2018). The Flood Control Act of 1936 called for further channel improvements and authorized construction of the Morganza Spillway upriver of Baton Rouge. The Morganza Spillway was designed to limit maximum flow downriver of this point at 1.5 million cfs (~42,000 cms) and can divert up to 600,000 cfs (~17,000 cms) (Lewis et al., 2018). The Morganza Spillway was not completed until 1954 and has only been operated twice—during large floods in 1973 and 2011. The 2011 flood in the LMR was the largest in the river since the Great Flood of 1927. It is important to note other large flooding events occurred on the LMR in 1945, 1950, 1973, 1975, 1979, 1983, 1997, 2002, 2008, 2011 and 2016-2020 (NOAA, 2019). Each of these flood events led to opening of the Bonnet Carré Spillway.

In 1929 the USACE began implementing an artificial cutoff program in the reach between Memphis, TN and Natchez, MS designed to reduce flooding and shortening navigation distances. When the program ended in 1942, 15 cutoffs had been constructed that shortened the LMR by 247 km between Memphis, TN and Red River Landing, LA.

This engineering effort has resulted in significant morphologic changes in this reach due to the increased water surface slope and stream power (Biedenharn et al., 2000). The increase in stream power has increased channel degradation in the cutoff reach and increased sediment supply and aggradation in downstream reaches that include Cat Island NWR (Biedenharn et al., 2000). The changing longitudinal profile of the channel bed and the confinement of the channel also have implications for river stage at a given discharge in the reach downstream of the cutoff program. Both of these engineering-induced alterations are expected to have impacted water and sediment delivery to downriver floodplains remaining in hydrologic connection to the channel (i.e., not confined behind artificial levees) including Cat Island NWR.

Large-scale engineering of the LMR in the vicinity of the Cat Island NWR study area continued with the construction of multiple water control structures at Old River Control Complex (ORCC) immediately upstream beginning in the mid-20<sup>th</sup> century (Figure 3). In the 1500s, the development of a meander in the MR allowed the Red River to flow into the channel and the Atchafalaya River to capture part of the flow of the MR as a higher-gradient path to the Gulf of Mexico (Weeks, 2016). Over time, the flow into the Atchafalaya increased to approximately 30% of total flow by the 1950s and the avulsion of the MR into the Atchafalaya became likely. As a result, the US Congress mandated construction of the first structure at ORCC to maintain MR flow down the Atchafalaya pathway at levels present in the 1950s. Flow to the Atchafalaya is fixed and adjusted daily using the ORCC structures at 30% of the combined latitudinal flow of the MR + Red River. Construction at ORCC was initiated in 1958 to create the Low Sill and Overbank structure, later supplemented by the Auxiliary Structure constructed in

response to near failure of the Low Sill structure in the 1973 flood. Since the flood of 1973, a navigation lock was installed at Old River to aid vessel transfer between the MR and the Atchafalaya and Red Rivers. Additionally, a dam and access channel were constructed at ORCC in 1991 upriver of the other structure access channels to generate hydropower (Weeks, 2016). Since the division of flow and sediment at ORCC was put in place, this has altered (reduced) flow volume and suspended sediment delivered to the Mississippi channel further downstream adjacent floodplain areas (Allison et al., 2012) including the Cat Island NWR study area.

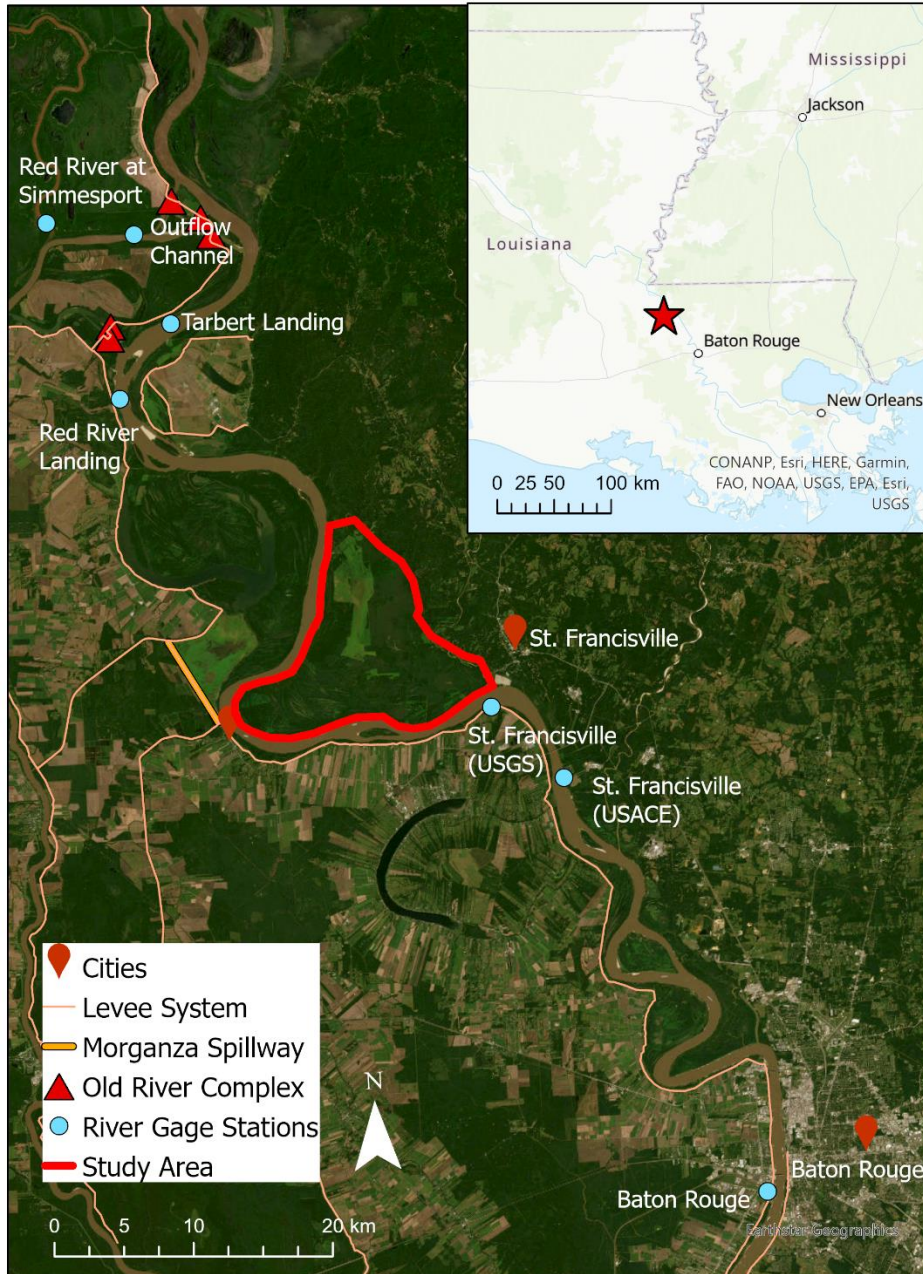


**Figure 3:** LMR from Old River Control Complex (ORCC) to Baton Rouge including the location of the Cat Island NWR floodplain study area, water and flood control structures at ORCC and Morganza, and the location of the US Geological Survey and US Army Corps of Engineers Mississippi-Atchafalaya River stage and discharge monitoring gages (modified from Myers, 2022).

Further engineering alterations to the LMR channel that have likely impacted sediment supply and floodplain connectivity includes the construction of concrete mat revetments along the entire LMR to reduce channel migration and further reduce dredging needs

(Moore, 1972). This has dramatically reduced migration-induced bank caving as a source of sediment to the channel, and potentially to floodplain areas that remain in hydrologic connection to the river (Murray and Biedenharn, 2022). Other potential impacts on sediment supply to the LMR floodplain include engineering conducted throughout the Mississippi Basin, most significantly including six reservoir dams constructed on the upper Missouri River tributary from 1933-1964 (Alexander et al., 2012). Dramatic declines in suspended sediment discharge in the MR after the 1950s have been ascribed chiefly to this damming, compounded by emplacement of revetments, wing dams, and soil conservation strategies in agricultural areas (Meade and Moody, 2009). The water control associated with damming in reaches above the LMR has also had the effect of reducing peak stage and discharge in large floods, increasing base (low) flow, and inducing overall shifts in the timing of low and high flow events reaching the lower basin (Alexander et al., 2012).

### 3. CAT ISLAND NWR STUDY AREA

The study area is a relatively natural area of the LMR floodplain of 38.9 km<sup>2</sup> that lies within the bounds of the Cat Island National Wildlife Refuge (NWR) downstream of ORCC and the Morganza Spillway and upstream of Baton Rouge, LA (Figure 3). The relatively pristine nature of the site is due to it being situated along a left-descending bank meander bend on the LMR that was not leveed in the MR&T program because it is bounded on the upland side by proximity to a Pleistocene terrace high ground that outcrops near St. Francisville, Louisiana. This results in the Cat Island NWR floodplain remaining subject to Mississippi overbank flooding in high discharge periods. Historical maps of LMR channel migration in the Cat Island meander bend (Figure 4) demonstrate that this floodplain bend has been relatively stable and not recycled by lateral channel migration for at least the last several hundred years. Cat Island NWR also contains the oldest baldcypress tree in the US, estimated at 800-1,000 years old, which also speaks to the stability of this floodplain area. The site's comparative stability and hydrologic connectivity to the channel—the refuge is inundated annually at Mississippi River stages above about 26 ft (8.2 m) on the Baton Rouge United States Geological Survey (USGS) stage gage—provides an opportunity to examine a relatively pristine remnant of the enormous area of floodplain that existed historically in the LMR basin. The present floodplain area is estimated at 27,000 km<sup>2</sup> (Murray and Biedenharn, 2022). Further, the widespread presence of baldcypress in Cat Island NWR, a species that is highly sensitive to seasonal and interannual changes in inundation with a positive correlation between water availability and growth (Kiem and Amos, 2012; Stahle et al., 2012; Therrell et al., 2020; Tucker et al., 2022), make this an exemplary site for studying the historical record

of LMR hydrology and the impact of engineering that has altered the flow and sediment load in the adjacent channel.

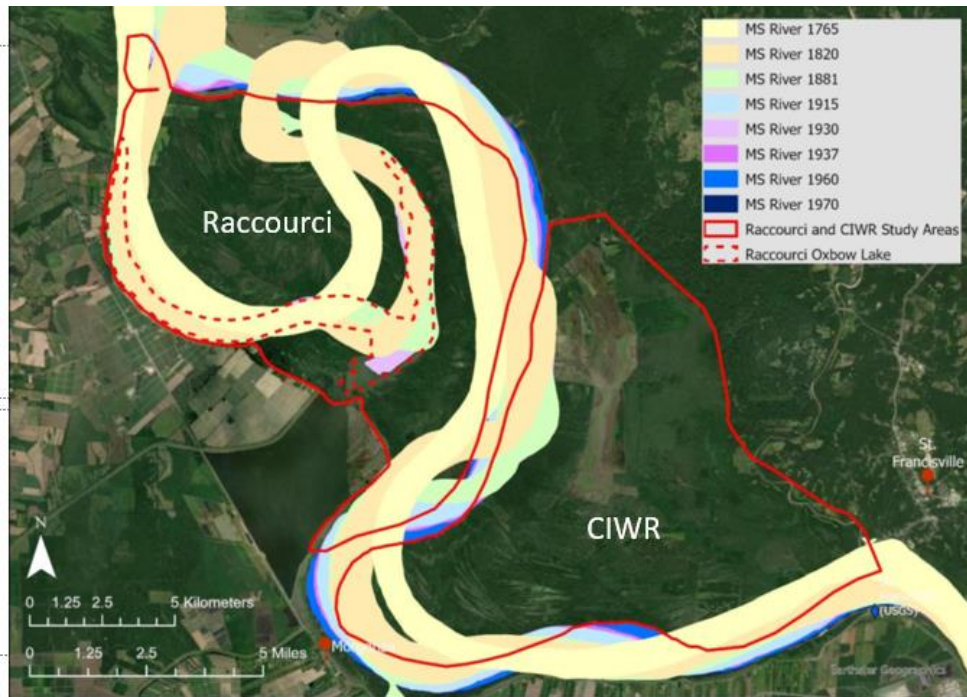


**Figure 4:** Migration of the Mississippi River channel since 1765 adjacent to the Cat Island NWR (CIWR) meander bend from historical maps of channel location (from Myers, 2022). The Raccourci area outlined on the right-descending bank refers to the Myers (2022) study that examined floodplain sediment deposition on both this and the CIWR side of the river.

The area between the channel of the river and the man-made levee is referred to as the floodplain. The floodplain is inherently connected to the river through overbank flooding events. Previous field investigations at Cat Island NWR found flood-high water marks from the 2021 annual inundation ~4m and above on trees (Myers, 2022). Annual inundation also inputs riverine suspended sediment into the floodplain: previous studies have suggested this floodplain between ORCC and Baton Rouge including Cat Island NWR is a large sediment sink for the suspended sediment budget of the LMR (Allison et al., 2012). Supporting this, Myers (2022) estimated from sediment depositional plots that

~10% of the LMR suspended sediment in WY 2021 was captured by the floodplain reach between ORCC and Baton Rouge.

Cat Island NWR becomes inundated annually by the higher stages in the adjacent LMR channel. Myers (2022) estimated that overbank inundation takes place when river stage at the Baton Rouge gage exceeds 8.2 m (26 ft.), although inundation and draining stage vary somewhat due to differing water surface slope on the rising and falling hydrograph.

Typically, the Cat Island NWR floodplain is inundated from approximately February to August (Figure 5). Myers (2022) utilized the approximate inundation stage, corrected for water surface slope, and the elevation of the deepest crevasses in the natural levee in the reach of the Cat Island NWR floodplain derived from LiDAR data, to calculate the duration of flooding throughout this floodplain bend of the river (Figure 6a). The correction for water surface slope to gauge overbank inundation was calculated by Myers (2022) at a mid-point channel (river) mile opposite the study area and was interpolated using river slope from LMR stage gages above (Red River Landing, LA) and downstream (Baton Rouge) of the reach.

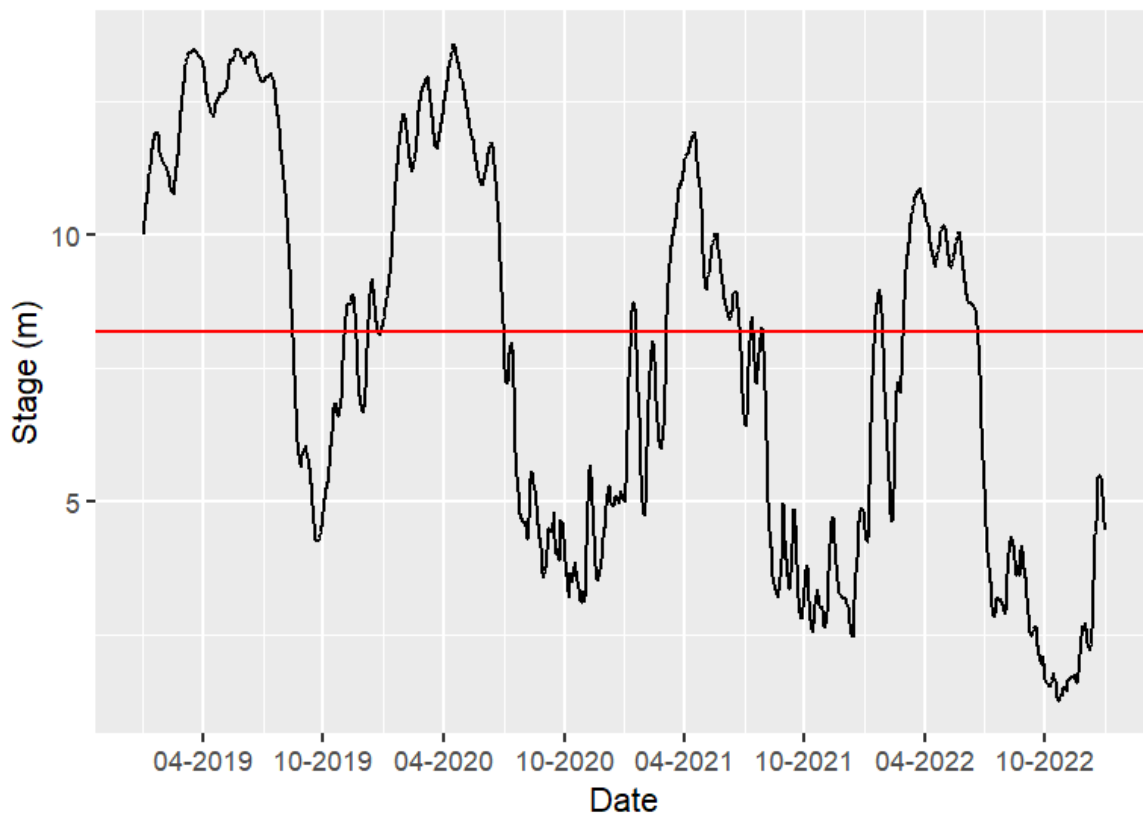


**Figure 5:** Daily Mississippi River stage at Baton Rouge, LA (USGS 07374000) spanning WY 2019 to 2022. The red line denotes the approximate river stage level at which overbanking water enters the Cat Island NWR study areas.

Maximum water depth in the Cat Island NWR floodplain in each WY can be calculated from these statistics by subtracting land surface elevation from the maximum recorded water stage recorded at the Baton Rouge gage. The duration of inundation is calculated by assessing stage frequencies above the necessary gage height to flood the study area. Depth of inundation in Cat Island NWR may vary significantly due to changes in elevation across the floodplain: microtopographic variations in elevation are common throughout this floodplain. Geomorphic features formed by later channel migration, such as ridges and swales, are characteristic of these environments. The highest elevations in the study area are typically found at the natural levee, in closest proximity to the river channel (Figure 6). Elevations generally become lower further inland from the channel as

shown in Figure 6b. These changes in topography are on the scale of centimeters to several meters but may provide notable changes to the environment, potentially resulting in variations in sediment deposition rates, water inundation duration and magnitude, and vegetation speciation.

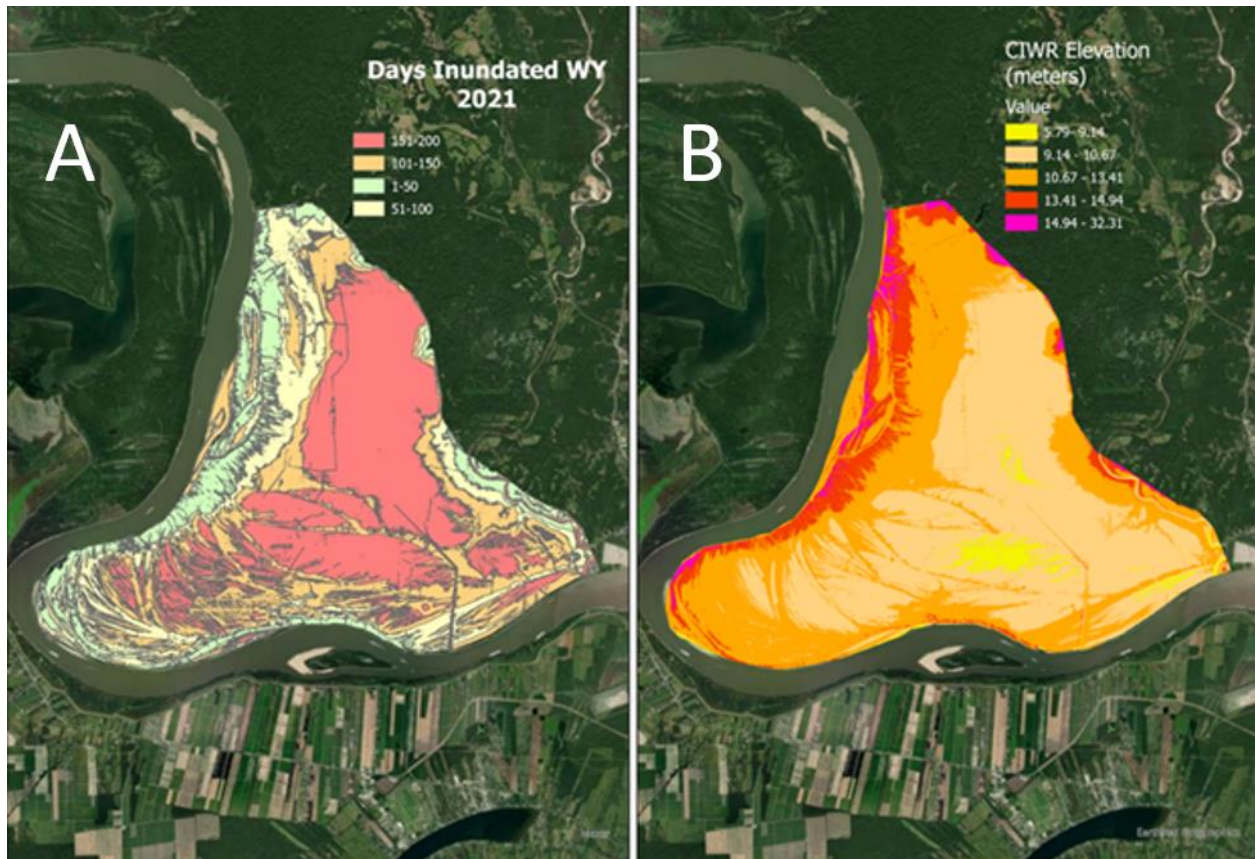


**Figure 6:** Calculated duration of inundation (A) for WY 2021 in days for the Cat Island NWR (CIWR) meander bend floodplain area based on river stage at Baton Rouge and the elevation of various areas of the floodplain (Myers, 2022). Elevation data (B) in meters from the Louisiana Statewide GIS obtained by airborne LiDAR (Louisiana Atlas, 2009; Myers, 2022).

The Cat Island NWR floodplain contains a wide array of tree species (Figure 7), including baldcypress and overcup oak, which have been used elsewhere in floodplains of the southeastern United States to track hydrological changes to the environment using dendrochronology (Therrell and Bialecki, 2015; Tucker et al., 2022). Baldcypress in the

Cat Island NWR is found primarily in lower elevations while overcup oak is typically found at slightly higher elevations within the floodplain (Figures 6b and 7). The change in species with changing elevation is potentially linked to inundation depths in floodplain areas. Given that low-elevation areas will be inundated to greater depths and for longer duration, they can be expected to support species that prefer wetter soils, such as baldcypress. Conversely, species that prefer dryer soils would be expected to be found in areas of higher elevation. The study area, delineated as a cypress-tupelo swamp by USACE (2023), is not dominated by these species. Baldcypress, black willow, hackberry, sweetgum, cottonwood and green ash together are the dominant tree species in the study area (Figure 7).

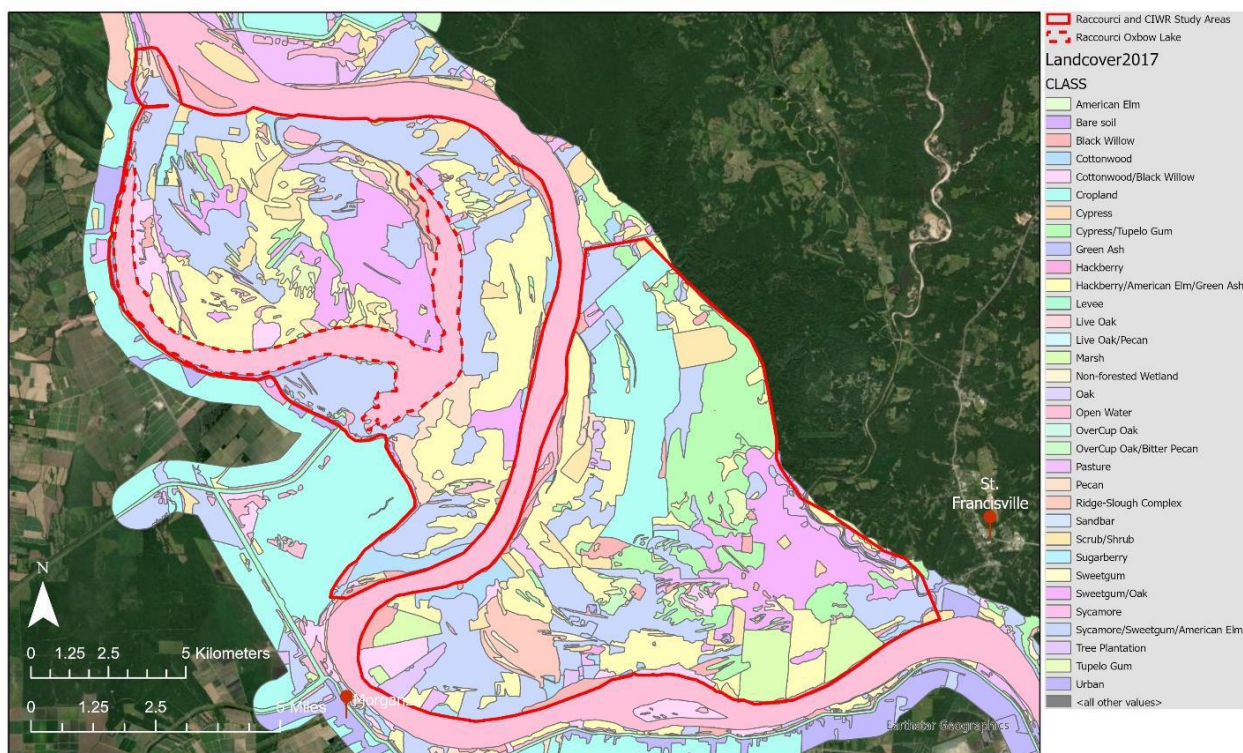


**Figure 7:** Predominant vegetation types in the Cat Island NWR floodplain which is the highlighted area in red on the left descending bank of the LMR (from USACE, 2019). The floodplain area on the right descending bank highlighted in red was an additional area of study (Raccourci) by Myers (2022).

## 4. METHODS

The focus of the present study is to utilize dendrochronological techniques to create a master chronology of baldcypress growth ring records in the Cat Island NWR to examine whether this chronology can be utilized to examine inundation of the floodplain in the study area. The dendrochronology reconstruction is supplemented with studies of water level in an individual flood at various sites in the Cat Island NWR and sediment studies that continue observations made by Myers (2022) into WY 2022. The sediment records provide a comparative WY record to the tree ring record.

### *4.1 Tree Coring*

Tree coring of baldcypress was conducted over as full a range of elevations and spatial extents as possible in the Cat Island NWR floodplain subject to constraints imposed by limits of baldcypress stands, logistical access, and the permitting within the NWR park boundaries. Tree coring does not harm the tree and is an effective way to collect tree ring data (Speer, 2012). Tree core locations were also selected to examine as wide a range of ground elevations and distances from the LMR channel as possible. While baldcypress trees are often located in lower-lying swamp elevations, the present study samples include higher relative elevations which may result from floodplain of greater age evolving to a higher elevation due to high sediment deposition sourced from the LMR channel. A total of 42 trees were sampled in the study area (Figure 8) with two cores collected per tree for a majority of the trees. The number of baldcypress trees sampled (42) allow for sufficient crossdating to occur so that a stand-level signal can be produced for the study area while reducing variability from any individual sample (Speer, 2012). Taking two cores per tree also permits crossdating in individual trees to improve

accuracy. Cores were collected using 5.15mm diameter Swedish increment borers of varying lengths. The length of increment borer used was dependent on the diameter at breast height (DBH) of the individual tree. Tree cores were taken at the visually estimated center of the tree in an attempt to include the pith (the center of the tree) in the samples. Coring for all samples was taken above the buttress of the baldcypress, with an average core height of 2.5 m above the ground surface. Cores were taken above the buttress to avoid aberration of growth based on tree morphology (Figure 9). Sample naming consists of a four-letter abbreviation for the species name, a two-digit number for the tree, and a letter for the core number within the tree. For example, TADI01B denotes the first baldcypress that was cored (i.e., 01) and the second core taken from this tree (i.e., B). Records of tree and site characteristics for all baldcypress cores are presented in Appendix A.

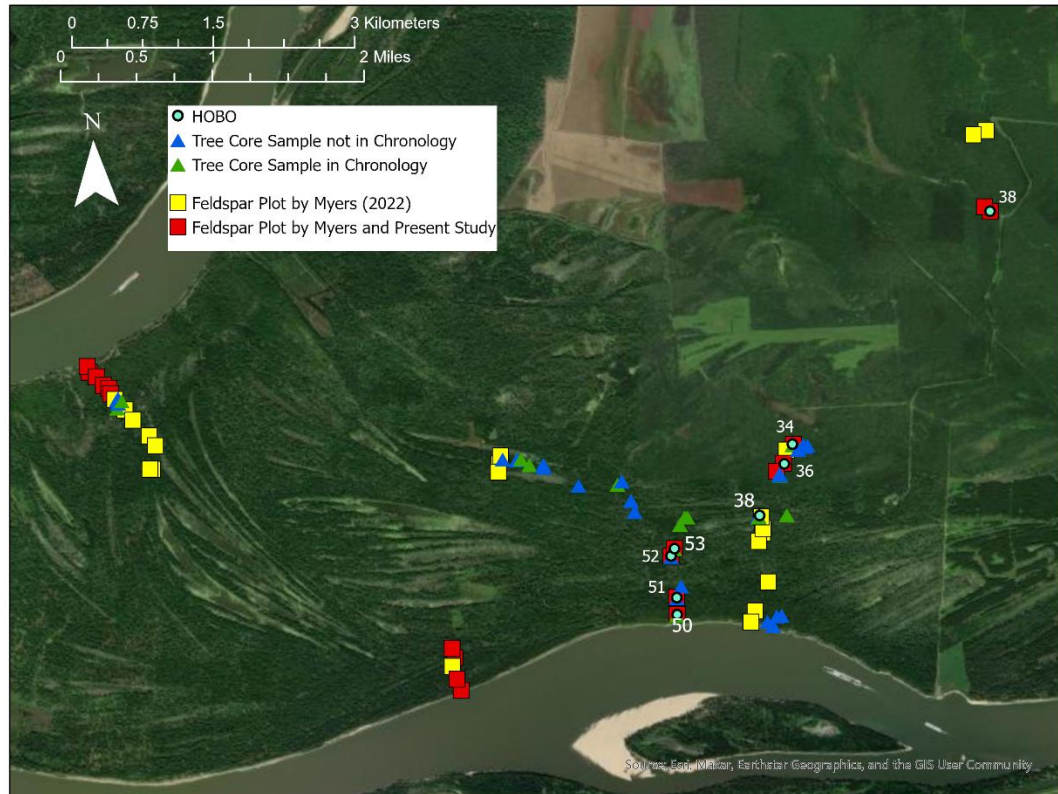


**Figure 8:** Field sample locations at Cat Island NWR for baldcypress tree cores, feldspar sediment deposition plots and HOBO water level loggers.

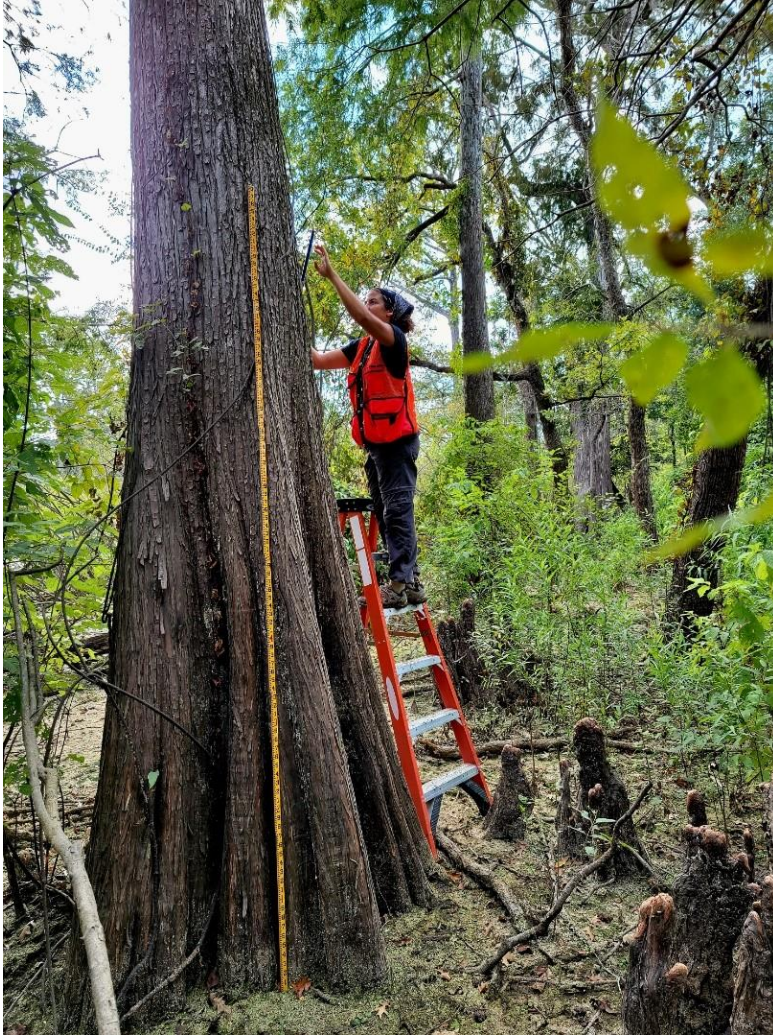


**Figure 9:** Coring a baldcypress in Cat Island NWR at a height required to sample above the buttress.

#### ***4.2 Tree Core Preparation and Analysis***

Cores from the baldcypress trees were mounted and sanded at 120, 400, 600 and 800 grit, respectively, using a random orbital hand sander and finished with hand sanding at 1000 grit. All cores were prepared and analyzed in laboratory facilities at the U.S. Army, Engineering Research and Development Center (ERDC) in Vicksburg, MS. Prepared core sections were then scanned at 2400 dpi using an Epson LA2400 scanner at ERDC for image analysis. Further examination and dating of samples were completed

using a combination of winDENDRO (Regents Inc., 2001), an imagery system for tree ring analysis, and a microscope for visual inspection. Ring width measurements were taken using winDENDRO. These measurements were read into RStudio to detrend and create a master chronology using the “dplR” package (Dendrochronology Program Library in R, Bunn et al., 2022). The cores were crossdated using the list method—a method used to verify dated tree cores by listing each thin ring year in a sample and correlating the occurrences of thin years to occurrences in other samples (Yamaguchi, 1991). Accuracy of crossdating was checked by statistically matching measurements of each core to the master chronology and a final chronology was created using COFECHA, a computer program for quality control of crossdating and measuring tree rings (Holmes, 1983; Speer, 2012).

#### ***4.3 Water Level Loggers***

Water level loggers were deployed at eight tree core sites within Cat Island NWR at various ground elevations and proximity to the LMR channel to examine flooding history for comparison with tree ring data (Figure 8). Onset, Inc HOB0 water level loggers were deployed on baldcypress knees or small trees at 10 cm above ground level in the December-March 2022 dry period prior to inundation by the 2022 MR flood. The loggers were set to record hourly data for atmospheric pressure when not inundated to aid in converting pressure readings to water depth levels. Loggers were recovered the following post-flood (August-October 2022) and used to create flood depth profiles using HOB0ware software.

#### ***4.4 Feldspar Sediment Deposition Plots***

Feldspar marker horizons (feldspar plots) were used to collect yearly sediment deposition measurements for potential comparison to the dendrochronology record. Methods in Kleiss (1996) were used to deploy feldspar monitoring plots of 50 x 50 cm initiated by Myers (2022) in August 2020- January 2021, and to deploy additional plots at additional locations matching locations where baldcypress were cored. Feldspar plots were deployed in the dry season (January-February 2022) and plots revised to collect deposition measurements were made once flood waters receded (Summer-Fall 2022 and November 2023-January 2024). Measurements of the total sediment deposition above the feldspar layer were made at three or more points within the feldspar plot to obtain an average deposition thickness for a site. Plots were marked by a 1-inch (2.5 cm) PVC pipe extending 1.25 m above the ground and coordinates were recorded with a GPS. For the monitoring of the plots initiated by Myers, the thickness of sediment deposition in these earlier WY was subtracted from the total deposition measured at the end of the WY 2022 flood to determine the sediment deposition rate in WY 2022 (see Appendix B).

#### ***4.5 Analysis of MR Historic Stage and Discharge Records***

Long-term hydrologic records of the LMR stage and water discharge were compiled (Table 1) and analyzed using RStudio for comparison to the baldcypress master chronology. The longest period of record stations for this reach of the LMR channel were selected and had records dating back more than 200 years. Daily stage data were obtained from the National Water Information System (NWIS) and the USACE (rivergages.com) websites (Table 1). USGS Baton Rouge, LA (Station USGS 07374000)

and Red River Landing, LA (USGS 07373290) are the closest sites to Cat Island NWR downriver and upriver, respectively, and were used to extrapolate yearly maximum stage, yearly duration of inundation, seasonality of peak stage, and the timing (seasonality) of inundation. The gage height datum used to reference stage at both stations is 0.00m NAVD88. Yearly maximum stage was obtained from the highest daily gage height reading. Duration was obtained from the number of days the daily gage height read above 7.4 meters (Baton Rouge) and 12 meters (Red River Landing). This height was found by the HOBO water level loggers as the lowest stage at which water was recorded entering Cat Island NWR (see Results section below). Seasonality of peak stage was obtained from the months associated with each yearly maximum stage record and a count of maximum occurrences in each month was created. Dates of inundation were recorded from the dates when the LMR gage height rose above 7.4 meters at Baton Rouge and 12 meters at Red River Landing.

**Table 1:** Data compiled for LMR hydrologic records in proximity to the study area.

<b>Station name and #</b>	<b>River mile and Elevation (NGVD29, m)</b>	<b>Data Compiled</b>	<b>Period of Record</b>
Natchez, MS USGS 07290880	RM363.3 5.27	Daily Stage Yearly Max Stage	1940-2022 1811-2023
Red River Landing, LA USACE 01120	RM302.4 0	Daily Stage Yearly Max Stage	1935-2022 1872-1978
Tarbert Landing, MS USACE 01100Q	RM306.3 0	Daily Discharge	1930-2022
Bayou Sara, LA USACE 01140	RM265.4 0	Daily Stage	1946-2015
Bayou Sara, LA USGS 07373310	RM265.4 0	Yearly Max Stage	1889-1978
St. Francisville, LA USACE 01145	RM260.3 0	Daily Stage	2009-2022
MR by St. Francisville USGS 07373420	RM266.0	Daily Discharge	Intermittently since 1943
Baton Rouge, LA USACE 01160	RM228.4 0	Daily Stage Yearly Max Stage Yearly Avg Discharge	1997-2022 1872-2021 2004-2022
Baton Rouge, LA USGS 0737400	RM228.4 0 (NAVD88)	Daily Discharge	Intermittently since 2004

Peak yearly stage data exists further back in time than daily stage (to 1811 at some LMR locations). This data was obtained from the USGS NWIS website for the Mississippi River at Baton Rouge; Bayou Sara, LA (USGS 07373310) and Red River Landing. Additional data was obtained on peak yearly stage from the USACE (Andrew Ashley and Melinda Pullman, pers. comm.) for the Mississippi River at Natchez, MS above the Old River Control. Peak yearly stage was in NGVD29 vertical datum for all stations and was converted to NAVD88 by applying a -0.2 ft adjustment. Plots for each parameter were generated to illustrate all stations where data was obtained. Data for peak yearly stage period of record from Natchez, MS were combined from two sources: 1901-2021 from

the Corps Water Management System and 1811-1909 from records of the Mississippi River Commission. The latter data is associated with a gage zero of 17.09 ft above Mean Gulf Level. The overlap of data between the two datasets gives the same readings, allowing a conversion for both datasets from NGVD29 to NAVD88 of -0.2 ft to be made.

## 5. RESULTS

### *5.1 Dendrochronology*

Core samples taken from 42 bald cypress trees between February 2022 and February 2023 in Cat Island NWR (Figure 8) were dated and cross-referenced to develop a location-specific dendrochronology. The tree core record from the Cat Island N group has a 113-year average between samples of annual growth ring record. Individual tree records date back to as early as 1849 based in annual growth rings, however, this is not representative of the exact age of all trees as many core samples were not taken to the pith, but it does speak to the length of record the trees can provide. Individual tree core chronologies are presented in Appendix A.

A total of 23 cores from 14 trees were selected to develop a final master (overall average) chronology representing approximately 1/3rd of tree cores sampled. These cores represent the full areal range of sampling (Figure 8, Table A2) and were selected based on their capacity for intercorrelation via crossdating. The difficulty of crossdating baldcypress trees due to their high sensitivity to water availability and their ability to produce false rings (as explained in Section 2.1), greatly reduces the number of cores from those taken in the field to those that remain in the final chronology. The final master chronology was truncated to the year 1900 as the expressed population signal (EPS) values were not acceptable for the earlier period of record. The series intercorrelation coefficient for the post-1900 record of 0.476 was acceptable (Table 2). This represents the average correlation of each series to the master chronology. The EPS for the chronology is 0.906 which was also acceptable. An acceptable EPS is defined as  $>0.85$  (Speer, 2012), and “acceptability” of a series inter-correlation is dependent on species

and study area characteristics with baldcypress chronologies commonly producing 0.4-0.5 series inter-correlation coefficients (Speer, 2012 and Clay Tucker, pers. comm.). The "dplR" package in RStudio was utilized to examine the ring width indices of the cores (Bunn et al., 2022). Correlations to the master chronology were done for 50-year segments, progressing through the series by half a segment length (e.g., 25 y) to find overall correlations. Segments are different sections of individual tree cores that are compared against one another to determine strength of inter-tree correlation. The chronology was detrended using a modified negative exponential model to eliminate long-term trends of decreasing ring width with age that are characteristic of typical tree growth patterns (Speer, 2012).

**Table 2:** *Descriptive tree ring statistics from Cofecha program output.*

Number of dated series	23
Master series length	123 yr (1900-2022)
Series inter-correlation	0.476
Average mean sensitivity	0.595
Mean length of series	101 yr

The final master chronology of the 14 baldcypress trees at Cat Island NWR that was built for the years 1900 to 2022 using the detrended series displays a high variability in year-to-year growth (Figure 10). Ring width index (RWI) varies by up to a factor of three from year to year in the chronology. Superimposed on the interannual variability in RWI is a broader period (running average line in Figure 10) of rising RWI after about 1940 that lasts until ~1995, after which RWI index begins to decline. Note that, prior to about 1965, the master chronology is based on fewer than the total 23 individual tree core chronologies that comprise the final master chronology and after this point it is based on

the total 23 (Figure 10). Years containing false rings were recorded for each series in the master chronology (Appendix A, Figure 11).

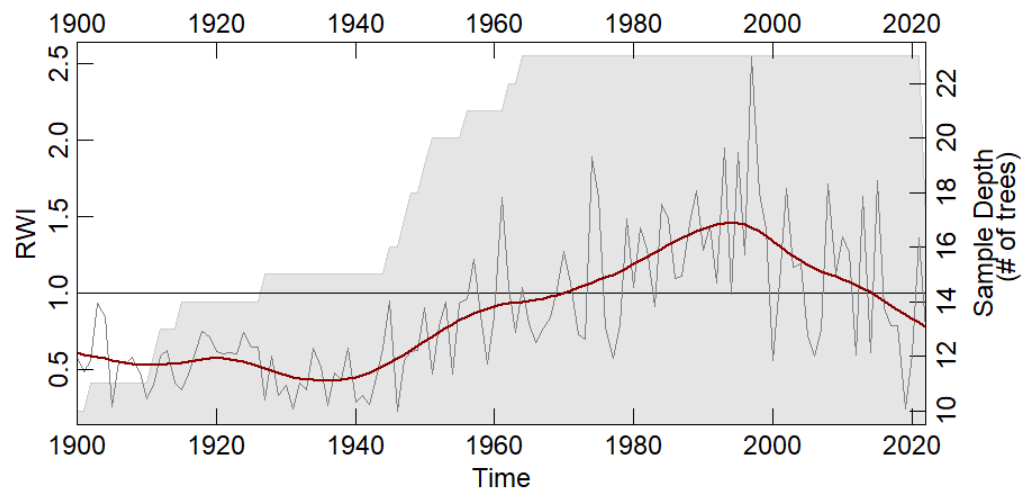


**Figure 10:** Ring width index (RWI) for the final master chronology from 23 tree cores representing 14 individual trees at Cat Island NWR derived from a modified negative exponential model. Sample depth is the number of trees that go into the chronology for each year depicted by the grey shading and is read from the right X-axis. A two-thirds smoothing spline average with a 50% frequency cutoff is depicted by the red line.

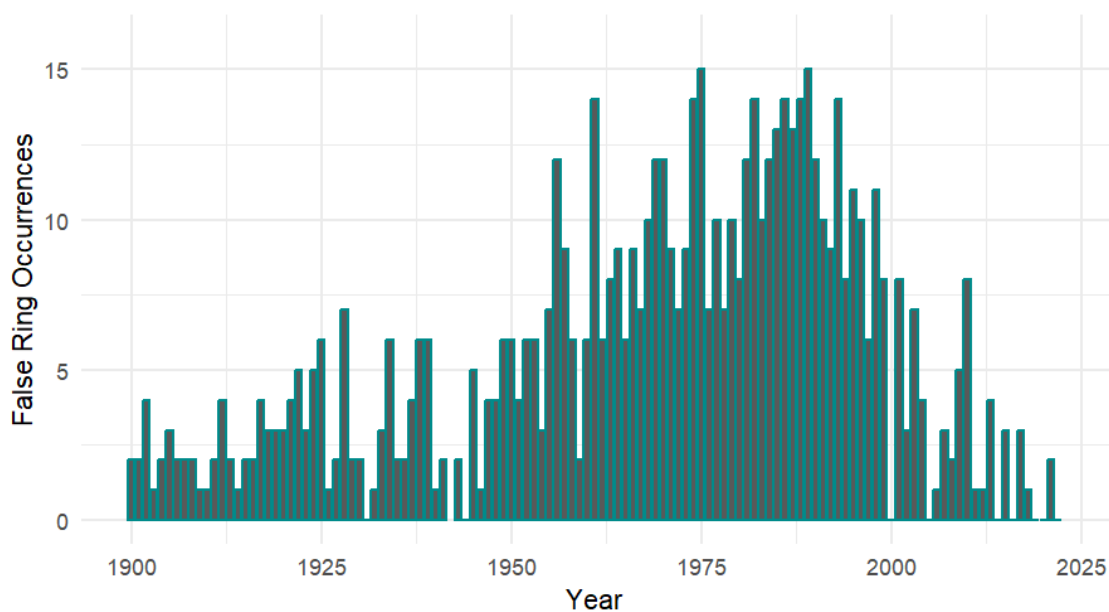


**Figure 11:** False ring occurrence in each year across the 23-core chronology.

## ***5.2 Floodplain Inundation at Cat Island NWR in Water Year 2022***

HOBO water level gages placed at eight locations within Cat Island NWR (Figure 8, Table 3) prior to the onset of overbank flooding in late February 2022 are a means to accurately determine the depth of flooding that sampled baldcypress trees experienced in the WY2022 flood. The NAVD88 elevation of each of these gages was determined using the LiDAR data shown in Figure 6 and is presented in Table 3. Error in the elevation of the HOBO location (Table 3) is derived from the range in elevation given by the LiDAR data (Myers, 2022). The varying water levels recorded depict how depth and length of inundation varied within the site in the WY2022 overbank flood into Cat Island NWR (Figure 12). In addition, one of the nine gages deployed in January-February 2022 was left throughout the WY2023 flood year (Figure 13) and provided an intercomparison of flood depths at the site (Station 36 in Figure 8) in two successive water years. The HOBOS deployed at locations further from the river (Figure 8) recorded that inundation occurred earlier, due to their lower elevation, and higher elevation stations flooded sequentially with the rising stage in the river channel. The highest elevation stations (Station 50 in Fig. 8) on the natural levee nearest the channel showed no flooding in WY2022. This indicates that flooding into the interior of the Cat Island NWR floodplain (and subsequent draining during the declining limb of the LMR hydrograph) was primarily through crevasses in the natural levee rather than overtopping the levee at this particular site. The HOBOS at lower elevations also recorded the greatest depths of flooding during the overbanking event that lasted from late February to late June 2022.

**Table 3:** HOBO water level logger elevations, coordinates, and deployment and collection date in the WY2022 deployment.

HOBO station #	Elevation (NAVD88, m)	Latitude	Longitude	Deploy Date	Collection Date
18	10.4 (+/- 0.3)	30.7584700°N	91.4804200°W	2022-02-14	2022-09-15
34	8.8 (+/- 0.3)	30.7651000°N	91.4763900°W	2022-02-14	2022-09-15
36	10.1 (+/- 0.3)	30.7632765°N	91.4773774°W	2022-02-14	2023-11-17
38	9.8 (+/- 0.3)	30.7864000°N	91.4531900°W	2022-02-14	2022-09-15
50	13.7 (+/- 0.3)	30.7493900°N	91.4900800°W	2022-02-14	2022-09-15
51	11.6 (+/- 0.3)	30.7510300°N	91.4900400°W	2022-02-14	2022-09-15
52	10.4 (+/- 0.3)	30.7550100°N	91.4904500°W	2022-02-14	2022-09-15
53	10.7 (+/- 0.3)	30.7557000°N	91.4900300°W	2022-02-14	2022-09-15

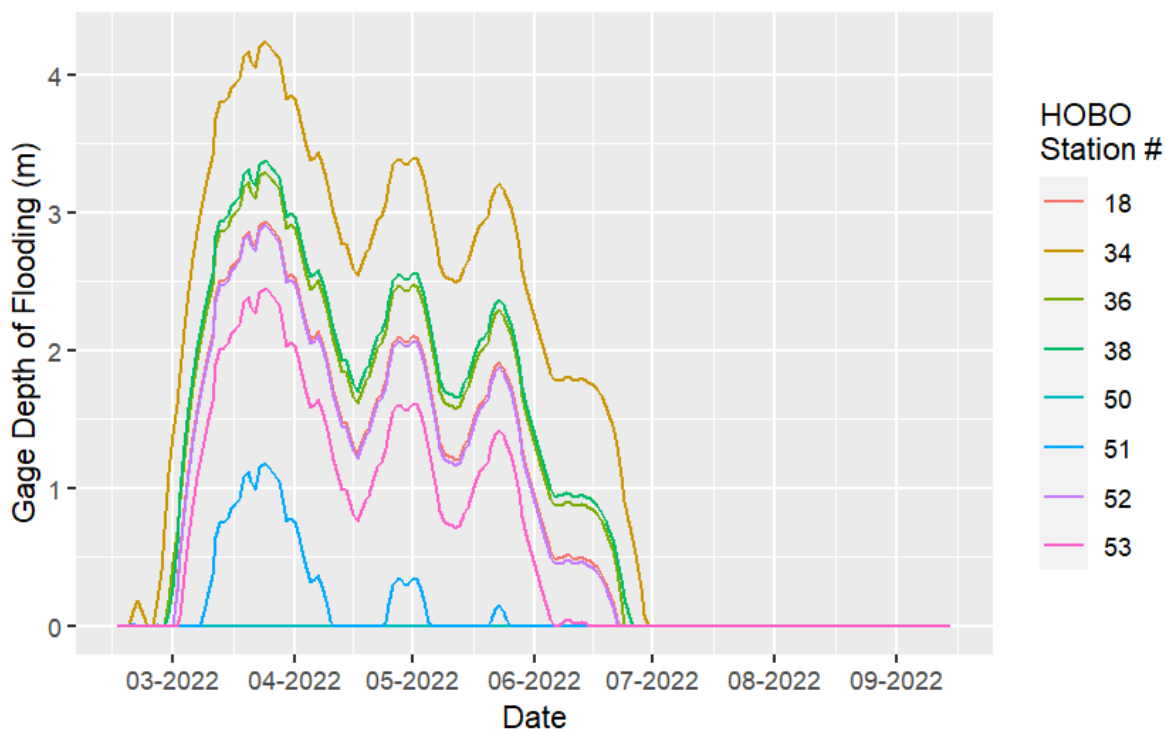


**Figure 12:** Depth of flooding recorded by individual HOB0 water level gages placed in Cat Island NWR during the WY 2022 overbanking event from the Mississippi River channel. Gages were deployed on February 14 and recovered on September 15, 2022 except Station 36 which was recovered November 17, 2023.

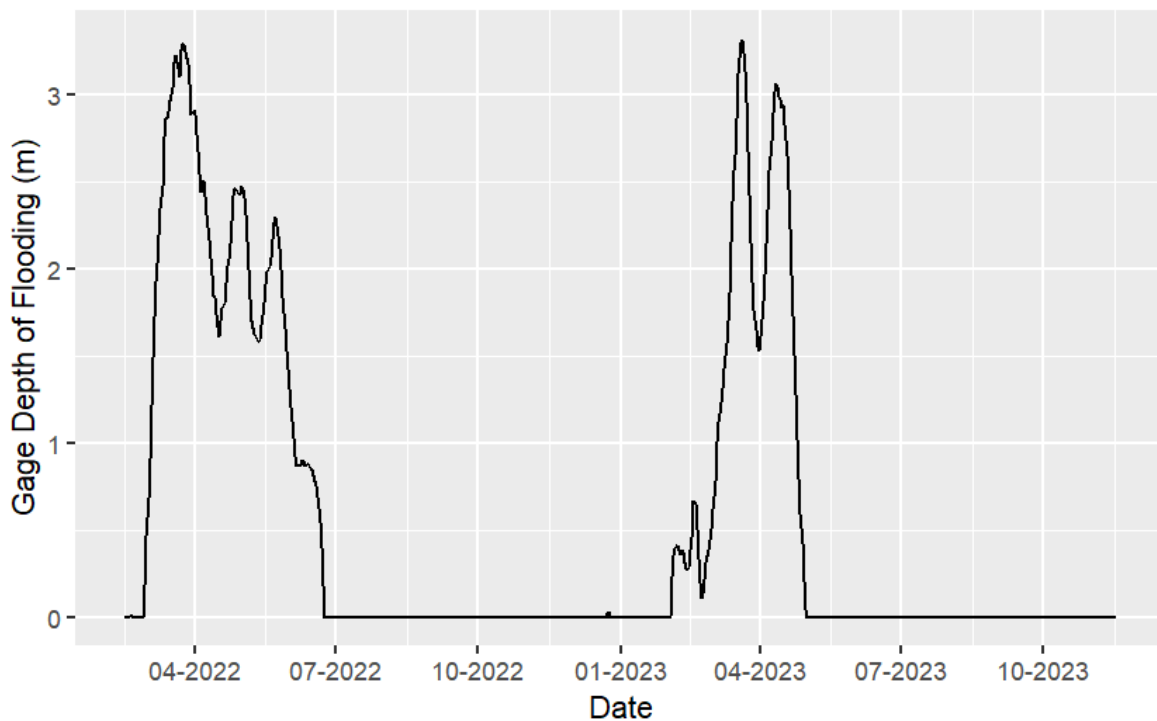


**Figure 13:** Depth of flooding recorded by HOB0 water level gage station 36 placed in Cat Island NWR during WY 2022 and 2023 overbanking event from the Mississippi River channel. The gage record serves as a comparison between the flood activity in the study area of the two WYs. Gage was deployed on February 14, 2022 and recovered on November 17, 2023.

The water surface derived from the HOB0 gages in WY 2022 largely mirror the hydrograph of the LMR as recorded at the monitoring stations at Baton Rouge, LA and Red River Landing, LA in that they record the timing and magnitude in stage variations in the March to late June period (Figure 14). The differences in stage recorded by the USGS stations at Red River Landing (RM 302.4) and Baton Rouge (RM 228.4) and the HOB0s in the floodplain are mainly due to water surface slope but also record a slight (<1 day) delay in arrival of the flood wave at Baton Rouge relative to the Red River Landing station upriver. Myers (2022) utilized a correction for water surface slope based on relative elevation of the two stations to estimate stage elevation at Cat Island NWR that would result in inundation of the floodplain.

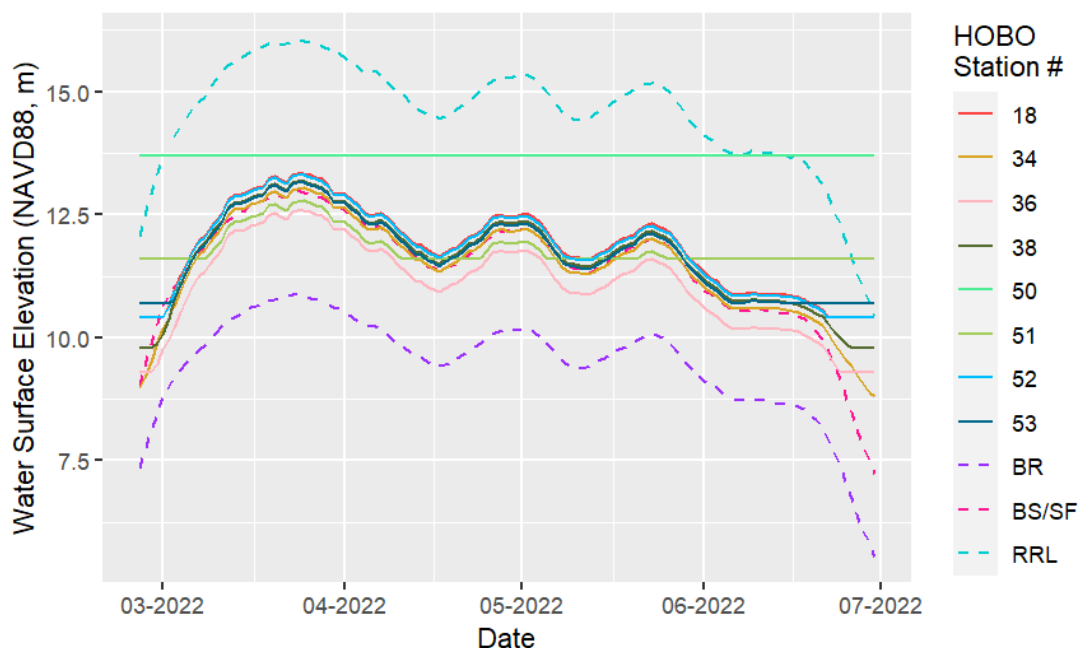


**Figure 14:** Water surface elevation calculated from LiDAR elevations and water levels above the gage recorded by HOBO water level gages placed in Cat Island NWR during the 2022 flood season. Water surface elevation is compared to water surface elevations for the USGS monitoring stations at Baton Rouge, LA, Bayou Sara, LA/ St. Francisville, LA and Red River Landing, LA. All elevations (floodplain gage and river) are expressed relative to NAVD88.

### 5.3 Mississippi River Historical Stage and Discharge

Historical records of LMR stage and discharge in the reach near Cat Island NWR were compiled (Table 1) and, where necessary, adjusted to modern vertical datums as outlined in the methods above, to facilitate an intercomparison with the baldcypress tree ring record. The daily stage data were manipulated to generate plots displaying various inundation information of the study area based on the flood heights determined by the HOBO water level loggers as explained in the methods section. Five USGS/USACE stations (Baton Rouge, Bayou Sara/ St. Francisville, Red River Landing, Tarbert Landing

and Natchez) were selected for this analysis based on length of record to compare with the 1900-2022 Cat Island NWR master tree chronology.

Daily stage records at Baton Rouge, LA, Bayou Sara, LA/ St. Francisville, LA and Red River Landing, LA show an increasing trend over the period of record (Figure 15). The seasonality plot (Figure 16) displayed that the occurrences of yearly maximum were recorded most from March-May according to all daily gage height records at Baton Rouge, LA, Bayou Sara, LA/ St. Francisville and Red River Landing, LA. All sets of data also portrayed an increase in yearly inundation duration at Cat Island NWR with more significant increases in maximum inundation than minimum inundation (Figure 17). All data sets for yearly peak LMR stage displayed high variability (Figure 18). Discharge data shows increases in recent years in both the Baton Rouge, LA and Tarbert Landing, MS stations (Figure 19). Further, days of inundation across the study area for WY 2022 were calculated using the slope of the river stage between Red River Landing and Baton Rouge to interpolate the water surface elevation at river mile 279, the midpoint of the study area (Figure 20). The days for which the water surface elevation exceeded the lidar elevation, depicted in Figure 6b, for any given area of Cat Island NWR are considered a day of inundation.

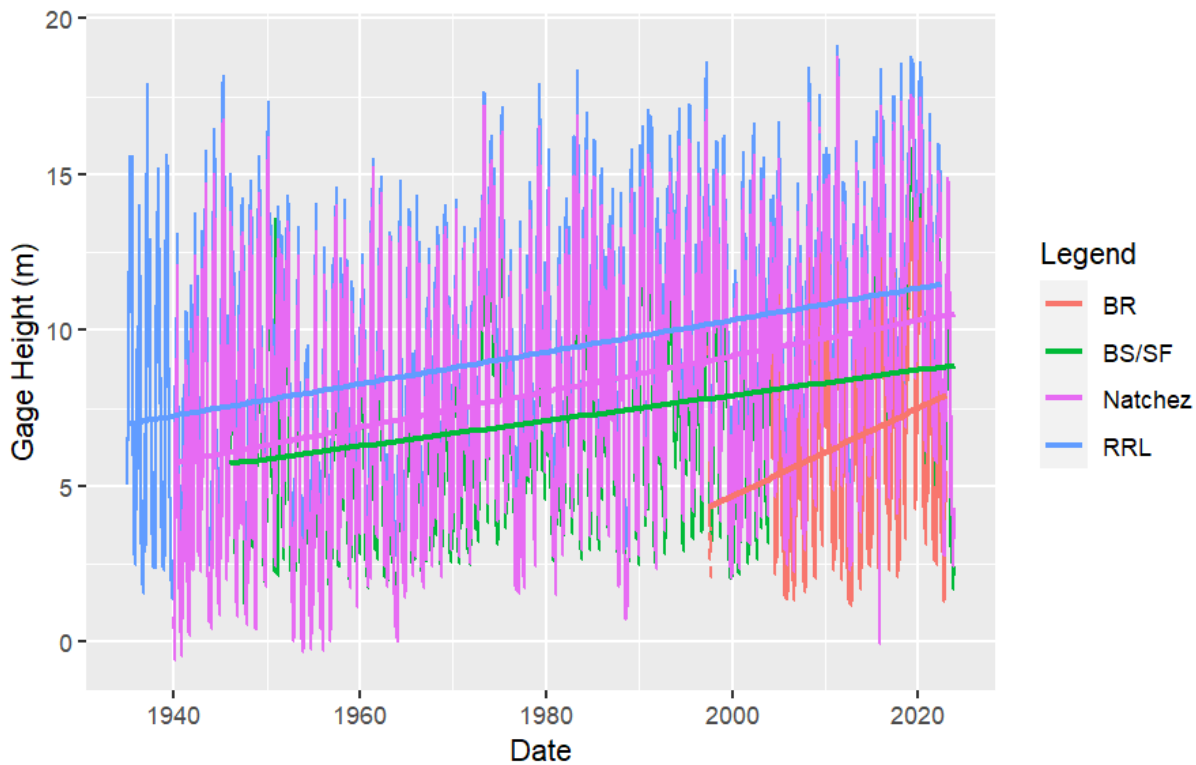


**Figure 15:** Daily stage records at USACE 01160 Baton Rouge, LA (BR), USACE 01140 Bayou Sara, LA/ USACE 01145 St. Francisville, LA (BS/SF), USACE 01120 Red River Landing, LA (RRL) and USACE 07290880 Natchez, MS. A best fit linear regression line is also shown for each station indicating an overall increase in stage over the period of record for all four stations.

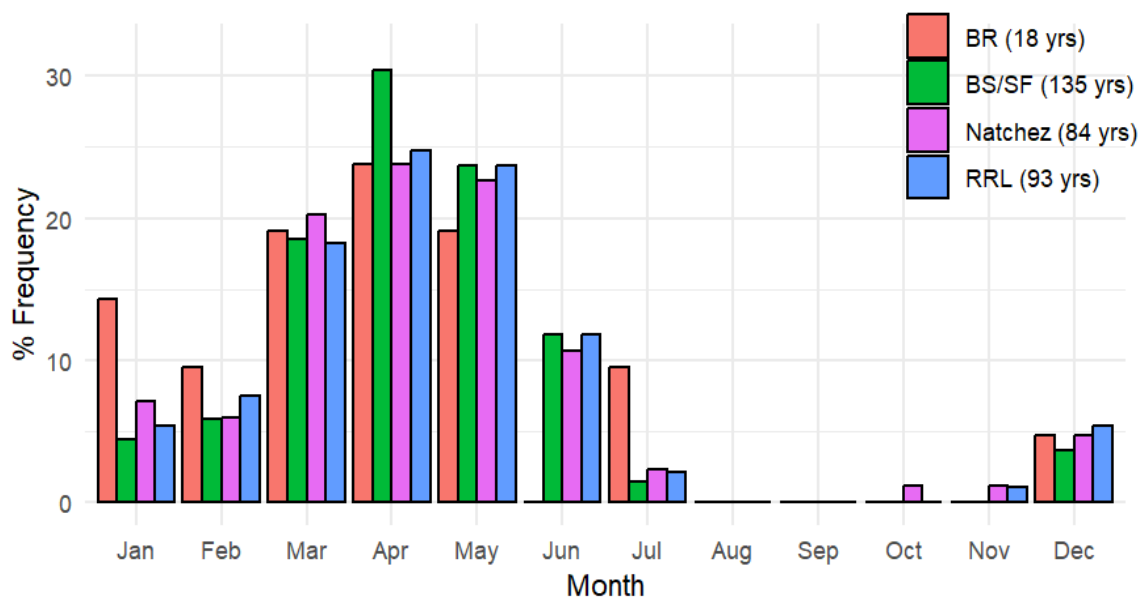


**Figure 16:** Peak stage seasonality at Cat Island NWR derived from daily stage elevation at USACE 01160 Baton Rouge, LA (BR) for years 2004-2022, USGS 07373310 Bayou Sara, LA/ USACE 01140 Bayou Sara, LA/ USACE 01145 St. Francisville, LA (BS/SF) for years 1889-2023 and USACE 01120 Red River Landing, LA (RRL) for years 1927-2022. Note that BS/SF data from 1889-1945 is from yearly peak data at USGS 07373310 Bayou Sara, LA recorded with day of occurrence.

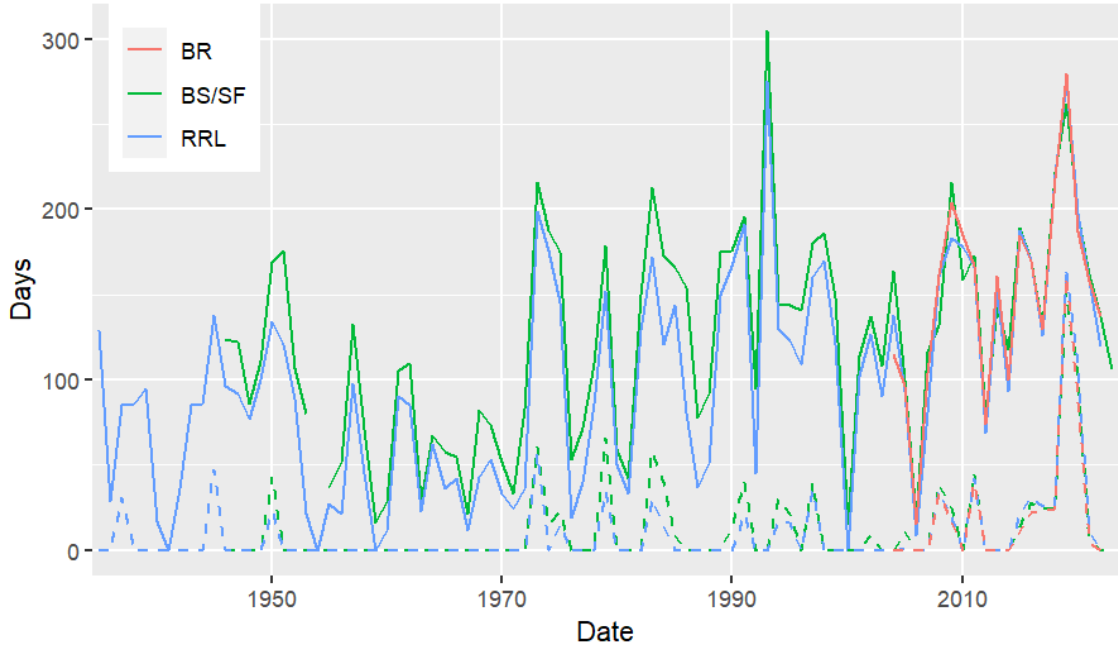


**Figure 17:** Maximum and minimum (dashed lines) days of inundation for each year at Cat Island NWR derived from daily stage data at USACE01160 Baton Rouge, LA (BR), USACE 01140 Bayou Sara, LA/ USACE 01145 St. Francisville, LA (BS/SF) and USACE01120 Red River Landing, LA (RRL). The maximum and minimum are derived from the maximum and minimum elevations of HOB0 water level gages in the study area. Days of inundation are calculated based on the number of days the respective gage is above the calculated gage height necessary to flood the maximum and minimum HOB0. The area in between the minimum and maximum lines is the estimated range of inundation for the study area.

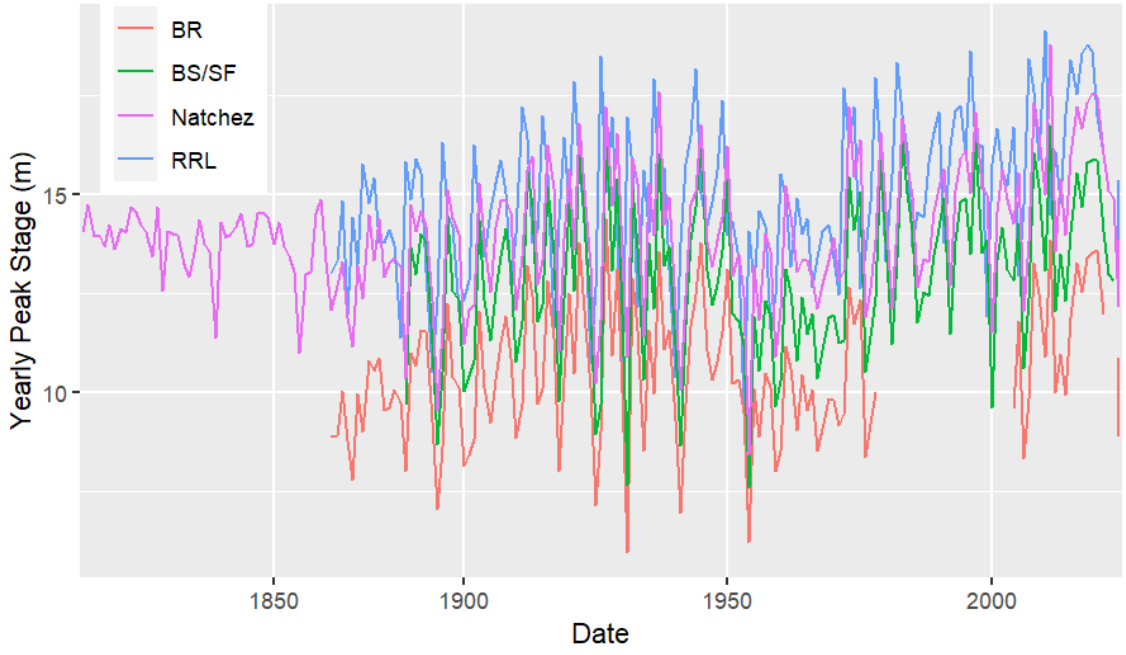


**Figure 18:** Yearly peak stage (NAVD88) of the LMR at USACE 01160 Baton Rouge, LA (BR); USGS 07373310 Bayou Sara, LA / USACE 01140 Bayou Sara, LA / USACE 01145 St. Francisville, LA (BS/SF); USACE 01120 Red River Landing, LA (RRL) and USGS 07290880 Natchez, MS.

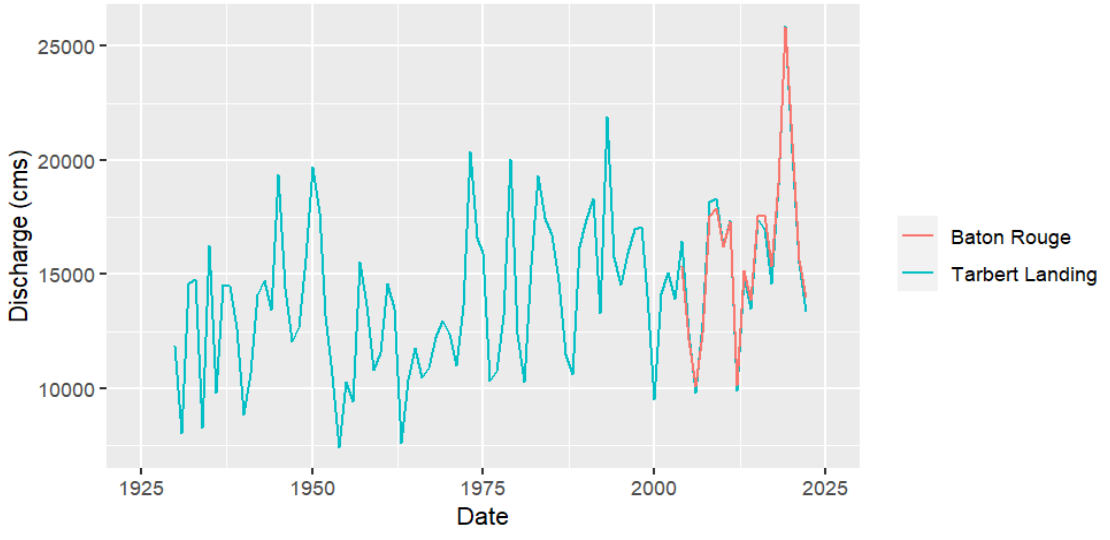


**Figure 19:** Yearly average Mississippi River water discharge at USACE01160 Baton Rouge, LA (BR) and USACE 01100Q Tarbert Landing, MS.

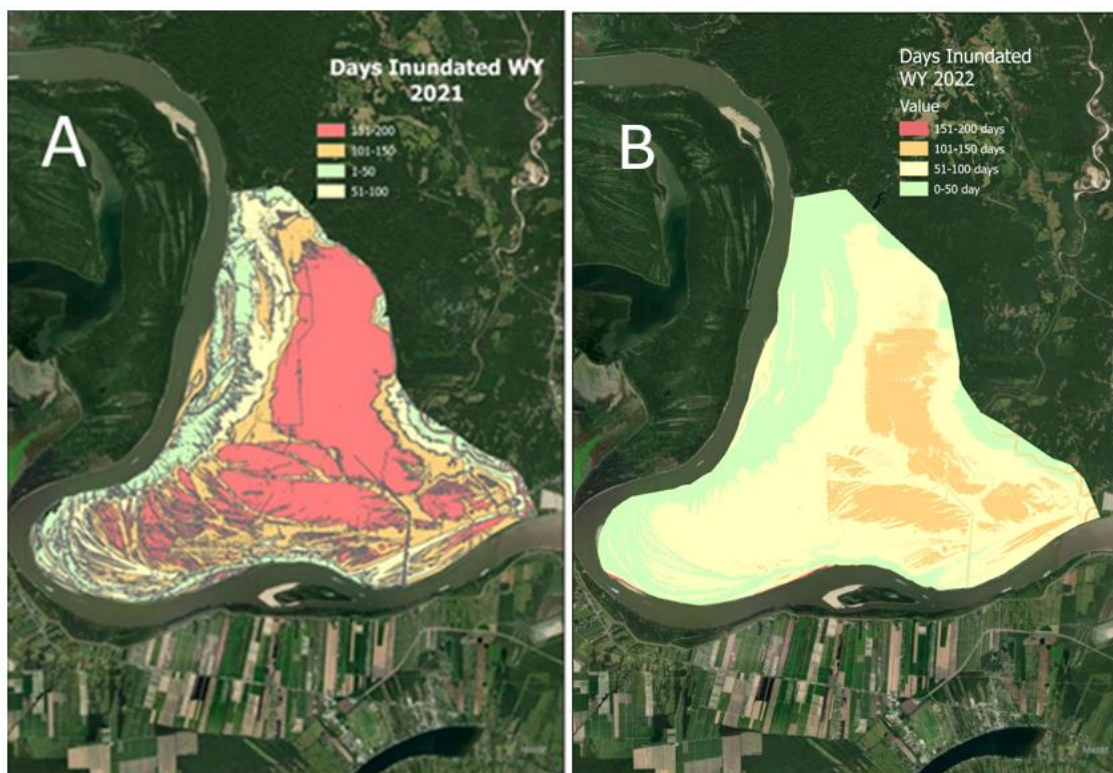


**Figure 20:** Comparison of days inundated at Cat Island NWR in (A) WY 2021 (from Myers, 2022) and (B) WY 2022. Note that the only days in WY 2022 inundated for 151-200 days are located in a small strip on the southern channel margin of the study area on the point of the meander bend, outside of the natural levee.

#### **5.4 Feldspar Plot Sediment Deposition in WY2022**

Sediment deposition data was collected at 19 feldspar plots in the Cat Island NWR floodplain in Summer-Fall 2022 that record sediment influx during the WY 2022 high water event. Deposition measurements ranged from 1.5 – 335mm (Appendix B). Deposition amounts were lower at almost all sites than those in WY 2021 (Figure 21) found by Myers (2022). The average amount of sediment deposition in the 15 stations measured by both studies decreased by 52% from WY 2021 to WY 2022. For years where measurements were made for all three years: WY 2020 had an average deposition

of 21 mm, WY 2021 had an average deposition of 50 mm and WY 2022 had an average deposition of 22 mm.

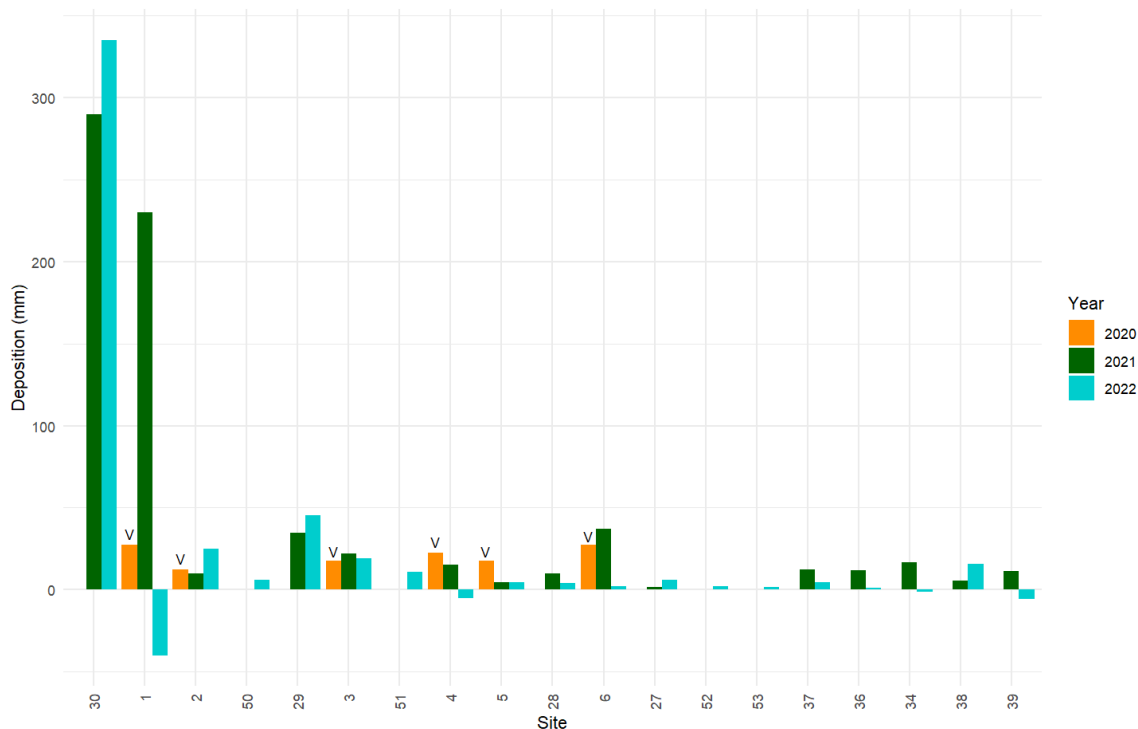


**Figure 21:** Annual sediment deposition rates in the floodplain at Cat Island NIWR for WY 2020, WY 2021 and WY 2022. WY 2020-2021 measurements are from Myers (2022). WY 2020 data was measured from depth of  $^7\text{Be}$  activity. WY 2021 and WY 2022 data were measured utilizing feldspar plots. The sites are ordered on the X axis in increasing distance to the river channel from left to right.

The deposition results show that varying amounts of sediment are delivered across the floodplain study area where measurements are recorded. Figure 21 shows a decreasing trend in sediment deposition at measurement sites with increasing distance from the river channel. Sites range in distance from 0.02 to 5.2 km from the river channel. It should be noted that Sites 1 and 30, which show the highest levels of sediment deposition (23 and 29 cm, respectively), are closest to the river and on top of the natural levee. Sites where erosional measurements occurred in WY 2022 are located over a range of distances from

the river and speak to high energies of water influx during the early overbanking phase that are capable of remobilizing the extant sediment surface. WY 2020-2022 sediment deposition rate data is presented fully in Appendix B.

## 6. DISCUSSION

### *6.1 Correlation with Individual Baldcypress Site Elevation*

As an initial step for understanding the sensitivity of baldcypress growth rates (as reflected in annual ring width) to elevation in the floodplain, growth rates were compared to site-specific durations of inundation and annual maximum inundation depth for individual sites. Correlations were calculated using Pearson product-moment correlation coefficient statistics and only computed for sample sites where both a HOBO water level logger and tree cores were collected. The presence of a HOBO water level logger gives a date at which the site received water and the depth and duration of inundation over WY2022. That site-specific record is then extended across previous flood years using the methods discussed in Section 4.5. River stages for site inundation utilize daily gage stage records at Red River Landing, LA. Maximum depth is quantified by using the differences in the WY 2022 maximum water surface elevation at Red River Landing, LA and the maximum water surface elevation of each HOBO record. These differences and individual HOBO site elevations are then utilized to adjust the maximum stage record at Red River Landing, LA over the period of record to estimate the maximum depth. All site-level correlation plots are presented in Appendix C and an example is shown in Figure 22.

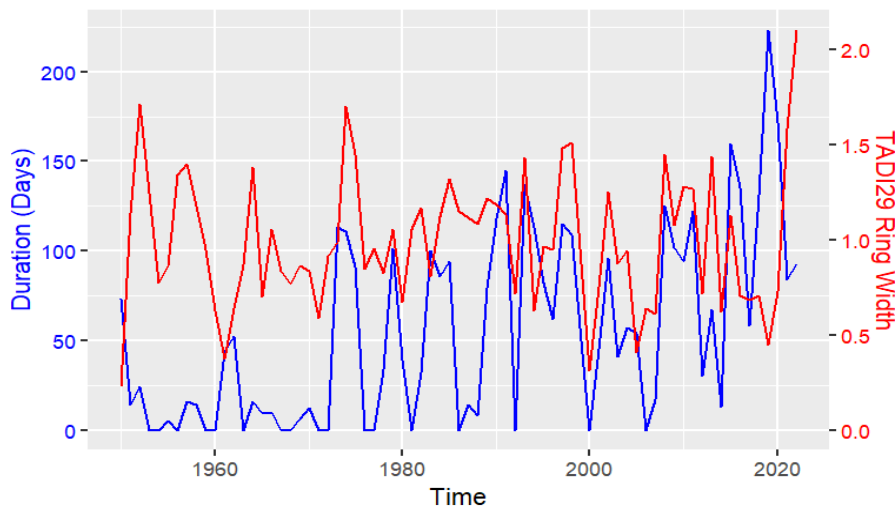


**Figure 22:** Example of the calculated duration of inundation at Site TADI29 (blue line) using the record of the HOB0 water level gage at the site (#18) to calibrate LMR stage at Red River Landing over the 1950-2022 period of record necessary to cause flooding. This is compared to the RWI at the site (red line). Site TADI29 Ring Width is an average of two cores from the same tree (TADI29A and TADI29B). Figures comparing other HOB0-tree core sites are presented in Appendix C.

The aforementioned statistical analysis suggests that elevation of individual trees was not found to be a driving force in tree growth rates when compared with inundation duration and maximum depth over the WY1950-2022 period of record. Correlations in all cases were low ( $r < 0.25$ ; Table 4). The range in elevation among the samples is 6.4 m. The low correlation of tree elevation in the floodplain to growth rates indicates that this range in elevation over the study area is not great enough to be a primary control on baldcypress growth rates. Likely this is because all the trees sampled are spread only along a LMR reach of less than 6 river miles (10 kilometers), and hence experienced very similar flood hydrograph timing, unlike trees growing along the entire 1,000-mile (1,600 km) reach of the LMR. Further, while maximum inundation depth differed by as much as 4 m (Figure 12) in the WY 2022 flood, the HOB0 records indicate that at all sites except the very highest elevation sites along the natural levee had inundation durations that differ by only a few weeks or less. Additionally, being in such close proximity means each tree site

experiences similar climatology. This verifies the approach for the method of tree core sampling used to construct the master chronology (Figure 10)—sampling across Cat Island NWR over a range of elevations, rather than in a more concentrated area. It also verifies utilizing a “lumped” strategy of examining interannual tree ring records as outlined below. Thus, the improved record for the Cat Island floodplain derived from averaging trees over a large number of stations (>20) shown in Figure 10 outweighs the differences imparted by elevation on the dendrochronology record.

**Table 4:** Elevation and river inundation statistics for individual sample sites in Cat Island floodplain where both a HOBO water level record and tree cores were collected. River stage for inundation is based on WY 2022 HOBO comparison with river stage at Red River Landing, LA. Inundation and maximum depth averages are for the 1950 to 2022 period of record. Pearson product-moment correlation statistics for duration of inundation ( $r_1$ ) and maximum flood depth ( $r_2$ ) to RWI are also for this period of record.

<b>HOBO Station #/ Tree Sample ID</b>	<b>Elevation (m)</b>	<b>River stage for site inundation (m)</b>	<b>Avg days/yr Inundation</b>	<b>Avg max Depth (m)</b>	$r_1$	$r_2$
34/TADI01	8.8 (+/- 0.3)	12.1	106	3.77	0.113	0.115
18 /TADI29	10.4 (+/- 0.3)	13.8	56	2.44	0.201	0.133
53/TADI12	10.7 (+/- 0.3)	14.0	48	1.97	0.233	0.235
50/TADI08	13.7 (+/- 0.3)	*16.7	10	0.340	-6.69e-04	0.047

\*Denotes estimated river stage at Red River Landing needed for site inundation as HOBO 50 did not become inundated in the 2022 flood.

## ***6.2 Baldcypress Chronology Correlation to Local Climatology***

In order to test the extent to which baldcypress tree ring indices correlate with local climatology as opposed to overbank flooding by the Mississippi River, temperature and precipitation records from the Systematic Remote Sensing and Computer Cartography (SRSCC) Laboratory for New Roads, LA were compiled for the period 1942-2022 (Table 5). New Roads, LA is located 9 km from the study area on the opposite side of the Mississippi River. The RWI dendrochronology comparison was carried out on the 23-tree average record (Figure 10). Correlation with the local average annual temperature record was low and inversely related ( $r = -0.21$ ). An inverse relationship is to be expected as baldcypress respond to elevated temperatures in the growing season by curtailing or ceasing annual growth (Stahle et al., 2012). The p-value is high ( $>0.05$ ) on this correlation, suggesting that the correlation may be due to chance and not significant. The p-value represents the probability that the correlation occurred by chance. A slightly better but still relatively low positive correlation ( $r = 0.31$ ) was found between annual precipitation and RWI. Positive correlation to precipitation is to be expected as water availability is one of the main drivers of baldcypress growth (Kiem and Amos, 2012; Stahle et al., 2012; Therrell et al., 2020; Tucker et al., 2022). In order to examine the extent to which local precipitation at Cat Island NWR has any link with LMR discharge in this reach of the river, Pearson's test was performed on the correlation between local precipitation and the water discharge record at Tarbert Landing, MS (Table 5). Results show there is a very low ( $r = 0.16$ ) correlation. This indicates that water levels in the LMR are primarily driven by basin-scale precipitation and runoff, i.e., wet years at Cat Island NWR do not necessarily correlate with wet years basin-wide that drive river level at the

site. Hence, it can be said that while local precipitation patterns do impact tree growth, it does not amplify relationships between LMR hydrology and tree growth. Minor feedback may be present in the floodplain during the falling LMR hydrograph when flood depth and timing of drying out may be impacted by high or low (higher evaporation) rainfall. Evaporation and transpiration are typically a large portion of water outflow budgets pertaining to drainage of flooded areas (Gulliver et al., 2010). This parameter that impacts timing of drying out is also linked to local temperatures and precipitation patterns.

**Table 5:** Pearson product-moment correlations of local climatological records (New Roads, LA) to ring width index (RWI) calculated for all trees at Cat Island NWR. Intercorrelation between precipitation and Mississippi water discharge at Tarbert Landing, MS. Red text rows are considered to have a statistical correlation relationship based on  $r > |0.2|$  and  $p < 0.05$ .

<b>Climatological Parameter</b>	<i>r</i>	<i>p</i>
Average Annual Temperature and RWI	-0.208	0.075
<b>Annual Precipitation and RWI</b>	<b>0.305</b>	<b>0.008</b>
Annual Precipitation and MR discharge	0.163	0.165

### **6.3 Baldcypress Chronology Correlation to Regional Climate Trends**

An intermediate scale (regional) of possible climatological links to baldcypress growth rates is climate indices over the southcentral US (Figures 23 to 25)—a scale still smaller than the Mississippi catchment (continental) scale that drives LMR stage and discharge and flooding at Cat Island NWR. As with the local climatology comparison (Section 6.2), the regional comparison concentrates on regional maximum daily temperature and the Palmer Drought Severity Index (PDSI). The maximum temperature used for this comparison is a time series from the Climate Research Unit Time Series climate dataset (Harris et al., 2020). PDSI is a measure of relative annual dryness based

on precipitation and temperature data from multiple regional stations and is obtained for the southcentral US from van der Schrier et al. (2013). The correlations shown in Figures 23 to 25 represent Pearson's  $r$  and results are interpolated from multiple stations across a six-state area around Cat Island NWR. A 100-kilometer circle around the study area is also shown to display the degree of correlation to stations in the immediate vicinity of the studied baldcypress.

The correlation between maximum temperature and RWI was averaged over three-month periods to examine any potential seasonal influence on the climatological linkage with dendrochronology. The strength of the negative correlation with maximum temperature varies depending on season (Figure 23). Maximum temperature in July-November shows the best correlation with baldcypress tree growth (RWI) at Cat Island NWR (Figures 23c and 23d) and has little or no correlation in the winter and spring seasons (Figures 23a and 23b). This corresponds to the senescent period for baldcypress in Louisiana (Egler, 1955). The best correlation is with the September-November period and may suggest that heightened temperatures during late summer and fall lessen or shut down baldcypress growth. This seasonally dependent negative correlation to temperature is found in every baldcypress chronology recorded thus far as indicated by Stahle et al. (2012). It is also evident that more distant station temperature records can be as well or better correlated to the RWI data than those within 100 kilometers. This may be a function that no station is located immediately within the Cat Island NWR floodplain and, hence, temperatures are as likely to be as closely related to these more distant stations when averaged at this broad seasonal scale.

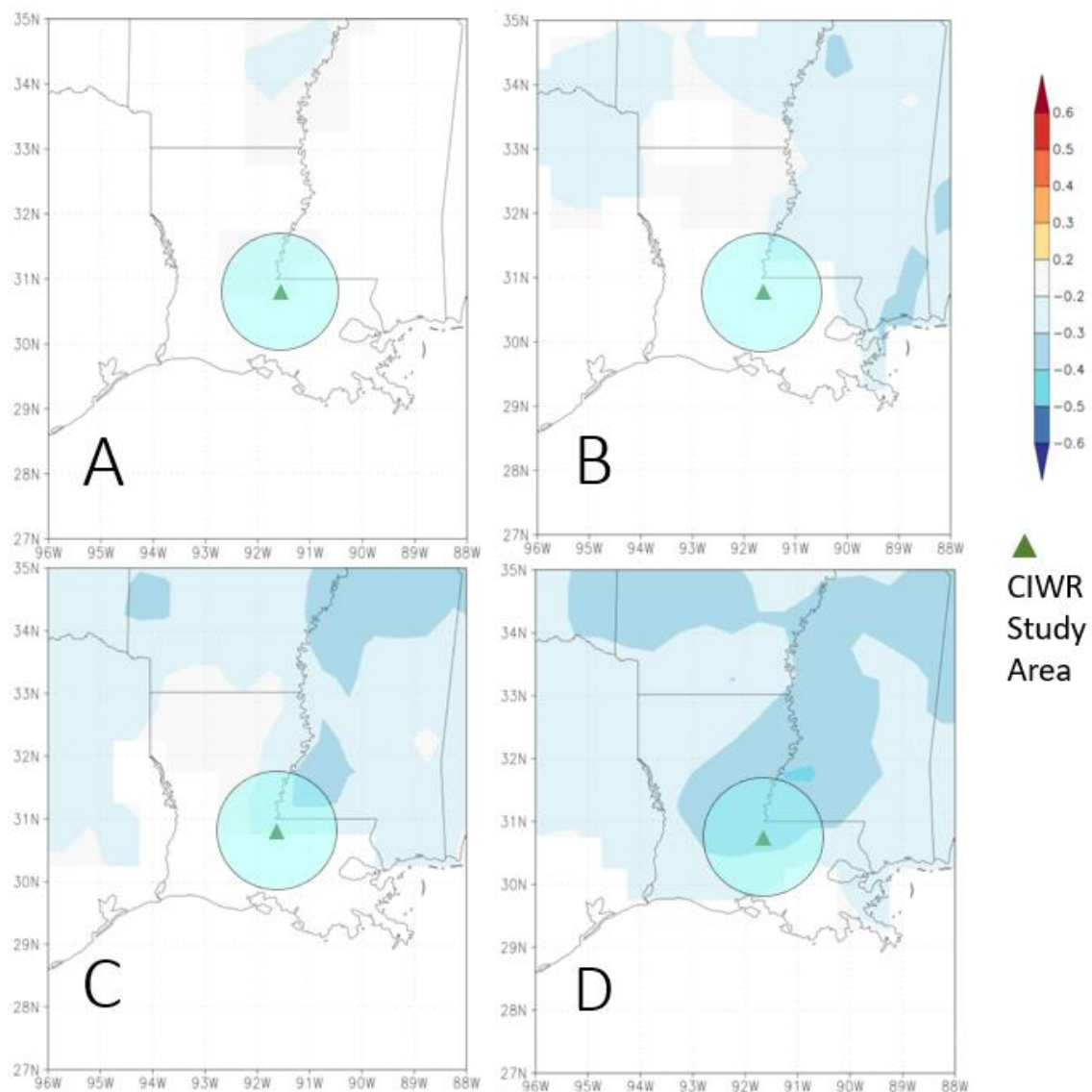


**Figure 23:** Maximum temperature Pearson's correlation to RWI (Harris et al., 2020). (A) Jan- Mar. (B) Apr- June. (C) Jul- Sep. (D) Sep- Nov. Figure 2D displays correlations for months Sep-Nov rather than Oct-Dec to depict the end of the growing season more accurately. The 100 km radius from the Cat Island NWR study area is contained in the shaded circle.

PDSI represents another potential linkage to the dendrochronological record and was averaged over annual (Figure 24) and three-month periods (Figure 25) to correlate with RWI. PDSI has been widely utilized by other investigators to correlate with baldcypress chronologies. Stahle et al. (2012), for instance, used Montezuma baldcypress to reconstruct PDSI over 1,200+ year tree ring record in Central Mexico. Positive

correlations between PDSI and RWI during the period when rainfall was monitored, were found during all seasons. Similar to the temperature relationship, the strongest correlation between PDSI and RWI in the present study was recorded at the end of the growing season (Figure 25d). The end of the baldcypress growing season in Louisiana is recorded as September (Eggler, 1955) although this may vary depending on timing of inundation recession (Stahle et al., 2012). However, the correlations throughout the individual seasons are comparable ( $r = 0.2$  to  $0.3$ ) for stations within 100 km of Cat Island NWR (Figure 25). The similarity of correlation coefficient between seasons may be due to high soil moisture availability in swamps (Deshpande et al., 2020); this suggests the trees are rarely stressed for necessary moisture even during very dry periods. As with maximum temperature, PDSI from more distant stations correlates as well or better than nearby stations (Figures 24 & 25), again potentially because there is no PDSI record from within Cat Island NWR. In summary, Figures 23 – 25 show some level of correlation to RWI for both PDSI and maximum temperature ( $p > |0.2|$ ), and hence, potentially complicate correlating RWI with the LMR hydrologic record (Section 6.4 below).

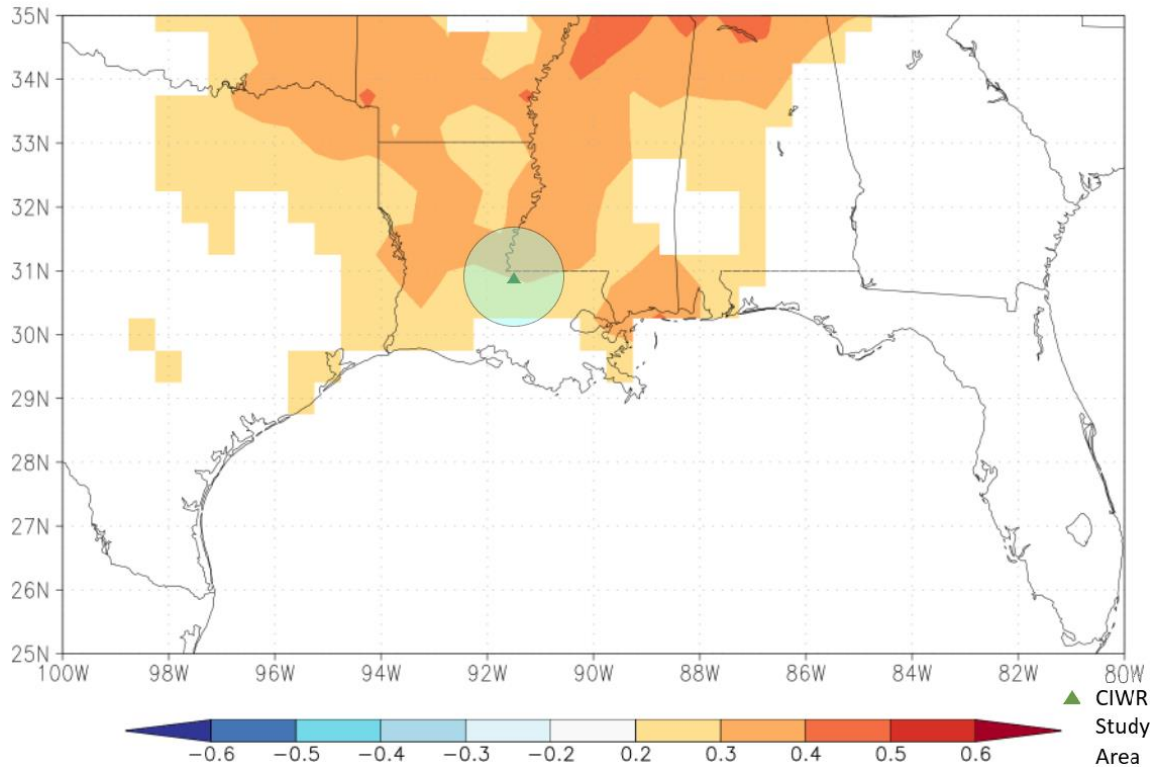


**Figure 24:** PDSI averaged over 1-year Pearson's correlation to RWI using the methods outlined in van der Schrier et al. (2013). The 100 km radius from the study area is contained in the shaded circle.

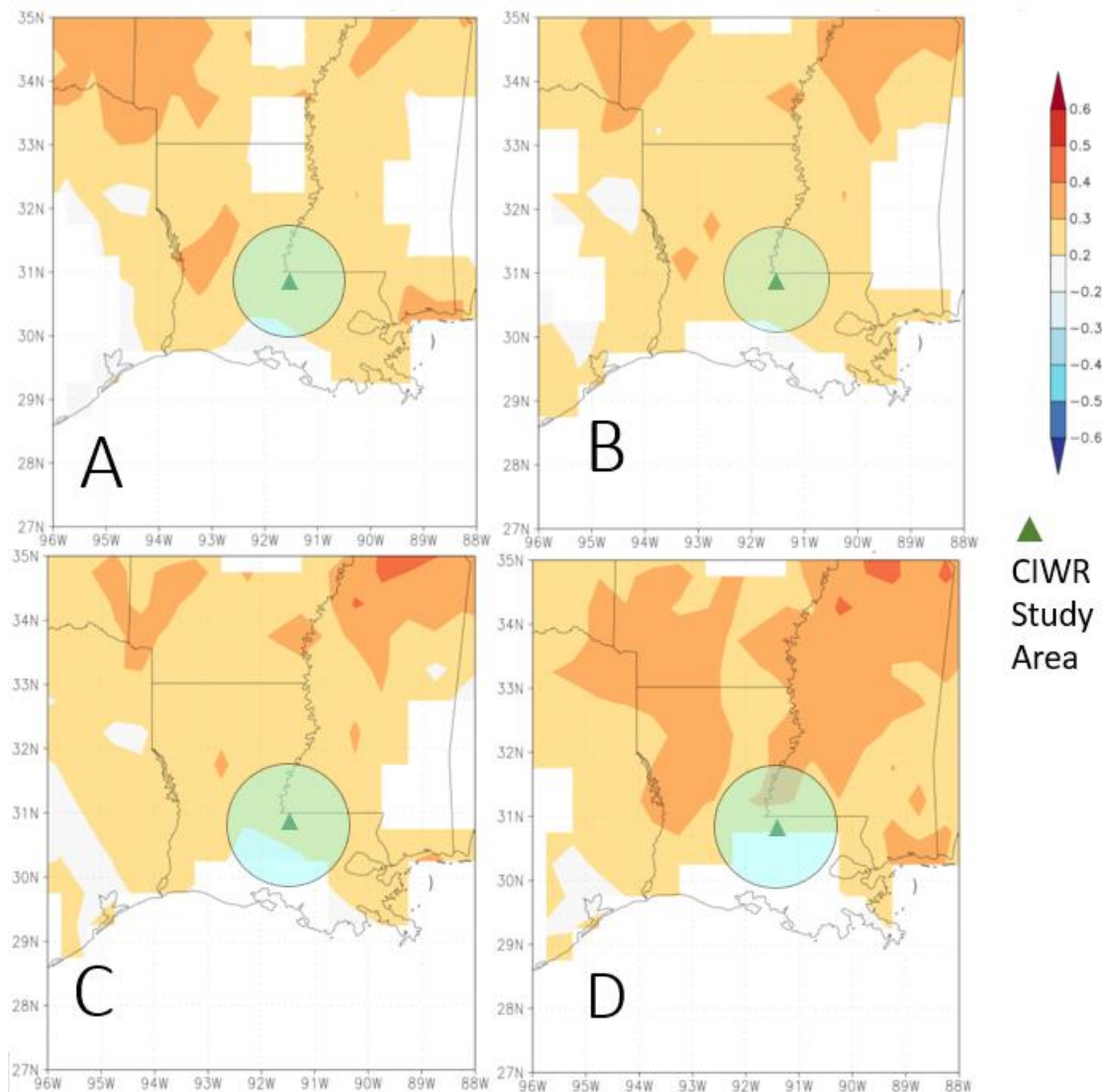


**Figure 25:** PDSI averaged over 3-month periods Pearson's correlation to RWI (van der Schrier et al., 2013). (A) Jan- Mar. (B) Apr- June. (C) Jul- Sep. (D) Oct- Dec. The 100 km radius from the study area is contained in the shaded circle.

#### 6.4 Baldcypress Chronology Correlation to LMR Hydrologic Records

Previous studies have suggested that there is a relationship between streamflow in adjacent rivers and baldcypress tree growth in studies from the Mississippi River basin (Therrell and Bialecki, 2015), and from other river catchments in the southeastern United States (Therrell et al., 2020; Tucker et al., 2022). To examine this linkage at Cat Island NWR, historical records from four LMR stations that monitor stage were used for

comparison to the dendrochronology in the present study. Since previous investigators have also used river discharge instead of stage to compare to dendrochronology records (Therrell and Bialecki, 2015; Therrell et al., 2020; Tucker et al., 2022), the nearest LMR historical discharge record (Tarbert Landing, MS) was also utilized. One river monitoring station (Natchez, MS) is located 84 river miles (135 kilometers) from the point of the Cat Island meander bend and is above the Old River Control removal of water down the Atchafalaya pathway. The others are 26 (Red River Landing, LA), 22 (Tarbert Landing, MS), 14 (Bayou Sara/St Francisville), and 52 (Baton Rouge) river miles (42, 35, 23 and 84 kilometers, respectively) from the meander bend point. Red River Landing is upriver (location of all stations in Figure 3) of Cat Island NWR but below ORCC. Historical trends for these sites are compiled for days/ year duration of flooding into the Cat Island NWR floodplain (Figure 17), yearly peak stage (Figure 18) and yearly average discharge (Figure 19). The Bayou Sara, LA/ St. Francisville, LA station, while immediately adjacent to Cat Island NWR, was omitted from the final statistical comparison with RWI (Table 6) due to the overbanking at this site on both sides of the river (Allison et al., 2012) and, hence, stage elevation is strongly controlled by loss of water to the floodplain. Table 6 summarizes the strength of hydrological correlation with the RWI from Cat Island NWR trees using three historical daily hydrograph records in the LMR as flooding parameters into the Cat Island NWR floodplain—duration of inundation, maximum stage/depth of inundation, and daily river discharge. Duration of inundation is calculated based on stage at the closest reliable stations above (Red River Landing, LA) and downriver (Baton Rouge, LA) of the study area (Table 6). Annual maximum stage is also compared for Natchez, MS.

The results of this statistical comparison of historical LMR hydrography with RWI in Table 6 show closer (direct) relationships ( $r = 0.33$  to  $0.43$ ) for several parameters (duration of inundation at Red River Landing, maximum stage at Red River Landing and Natchez, and river discharge at Tarbert Landing) than that displayed for local or regional climatology (see Sections 6.1 to 6.3 above) for the 1900 to 2022 period of record. These direct positive correlations demonstrate the controls of water availability on tree growth and baldcypress dependencies on MR for water availability in the study area. Pearson product-moment correlation coefficients are shown for each of these relationships in Table 6. Pearson outcomes with  $r > |0.2|$  and  $p < 0.05$  are assumed to be linearly correlated. All relationships in Table 6 were confirmed to be linear by plotting the data for each correlation in X-Y plots as exemplified in Figures 25b and 26b. Details of these relationships for the three river gaging parameters are discussed in the following sections.

**Table 6:** Pearson product-moment correlation coefficients for RWI and long-term LMR hydrologic data with their period of record. Red text rows are assumed to be linearly correlated based on  $r > |0.2|$  and  $p < 0.05$ .

	$r$	$p$	Period of Record
Duration of Inundation at CIWR based on RRL*	0.433	2.563e-05	1935-2022
Duration of Inundation at CIWR based on BR**	0.157	0.5202	2004-2022
Maximum Stage at Red River Landing, LA	0.398	1.24e-04	1935-2022
Maximum Stage at Baton Rouge, LA	0.179	0.577	2004-2022
Maximum Stage at Natchez, MS	0.332	1.79e-04	1900-2022
Discharge at Tarbert Landing, MS	0.353	0.0005154	1930-2022
Discharge at Baton Rouge, La	0.008	0.9728	2004-2022

\*Denotes data based on gage height readings at Red River Landing, LA.

\*\*Denotes data based on gage height reading at Baton Rouge, LA.

#### *6.4.1 Correlation with Duration of Inundation*

Duration of inundation is not traditionally studied as a driver of tree growth (Therrell and Bialecki, 2015). Baldcypress growth has been shown to increase with increasing water availability (Therrell et al., 2020 and Tucker et al., 2022). Duration records may give a more accurate assessment of water availability to the baldcypress in the growing season since water availability is unlimited during the inundated period in the floodplain and the earlier portion of the Spring-Fall growing season is under these conditions. Table 6 demonstrates that the flooding duration has the best relationship ( $r = 0.433$ ) of the hydrological parameters, with significant linear correlation at Red River Landing, LA (Figure 26). Lower correlation coefficient values are present for the gage at Baton Rouge, LA for duration, maximum stage and discharge: this may be attributable to the short period of record for this site (2004-2022) to test correlation with RWI.

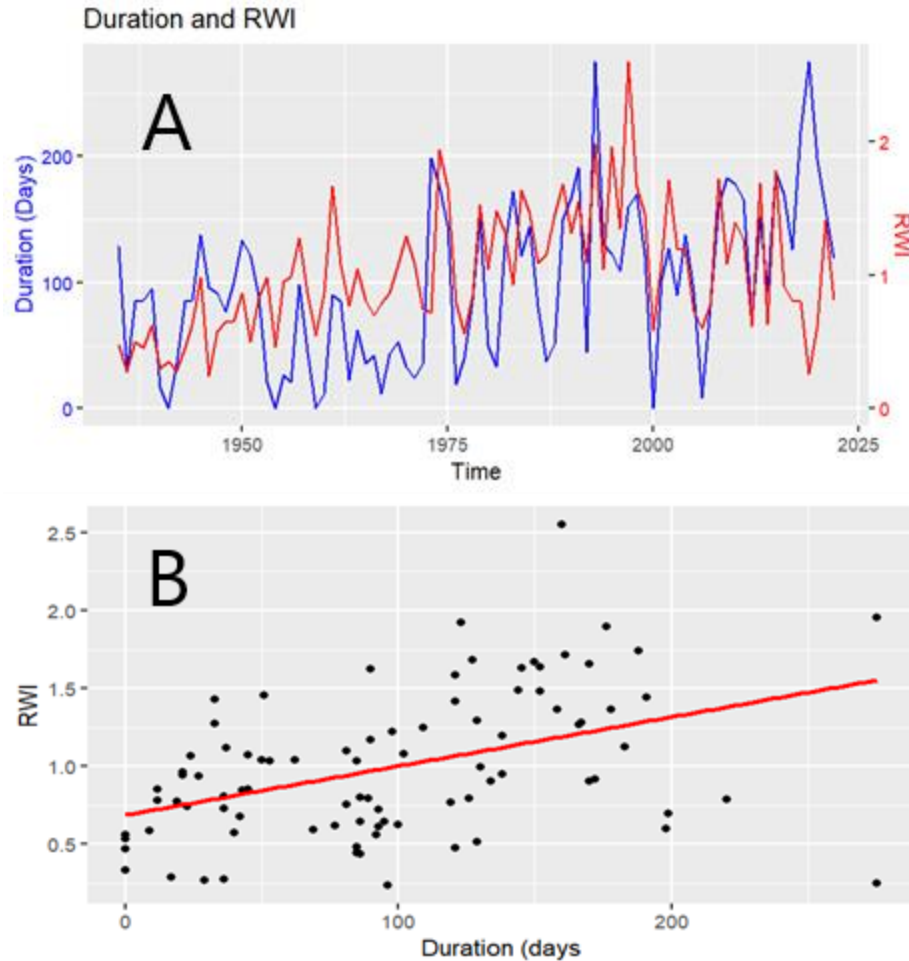


**Figure 26:** (A) Duration of inundation at CIWR based on gage height readings at Red River Landing, LA compared to RWI. (B) Best fit linear regression (red line) between these criteria

The observed positive correlation between multiple indicators of water availability derived by overbank flooding and RWI in the present study (Figure 26), is in agreement with previous investigators demonstration of the relationship between baldcypress growth and hydrology in other river catchments of the southeastern US. It should be noted that areas of lower elevation may receive higher water levels, but do not have significantly higher duration of inundation. This can be observed in Figure 13 that shows that the HOBO water level loggers have similar lengths of inundation and drainage time across the study area. Additionally, these areas do not retain significant water levels for more

than a few days after MR river stage has receded below elevation necessary to inundate Cat Island NWR. In WY 2022, the gage at Red River Landing dropped below the previously calculated flood stage for Cat Island NWR (12 meters, see Section 4.5) on June 25, 2022 and the last HOBO water level logger to record flooding reached 0.00 meters on June 30, 2022. Further, there is previous work that suggests baldcypress growth can be restricted after long periods of inundation and stratification of dissolved oxygen (Stahle et al., 2012). However, this is recorded in baldcypress in backwater swamps characterized by perpetual stagnant water conditions and inundation durations that span periods of several years. As baldcypress at Cat Island NWR likely experience periods of subaerial exposure lasting at least several months every year based on LMR stage records and the WY2022 direct observations of water level in the floodplain, they are not likely to experience stress to the point of hindering growth from prolonged flooding. The ability to endure this length of flooding is unique to baldcypress as other species' growth will typically shut down if inundated for the durations observed at Cat Island NWR (Kiem and Amos, 2012; Stahle et al., 2012; Tucker et al., 2022).

#### *6.4.2 Correlation with Maximum Stage*

As noted in above and in Table 6, positive (direct) correlation between RWI and maximum stage was found at all three LMR river gaging stations examined, albeit at a slightly less robust relationship than duration of inundation (Table 6). This correlation was statistically significant for Red River Landing, LA (Figure 27a) and Natchez, MS with the poorest relationship with the short record at Baton Rouge, LA. In all cases, the relationship was linear (Figure 27b) which confirms the use of Pearson's correlation coefficient for examining the relationship. Natchez is likely less well correlated than Red

River Landing as it is located above ORCC. The non-linear removal of water at ORCC, calculated daily at 30% of the latitudinal flow of the Red + Mississippi Rivers into the Atchafalaya, induces a variation not present at Red River Landing closer to Cat Island NWR and below ORCC.

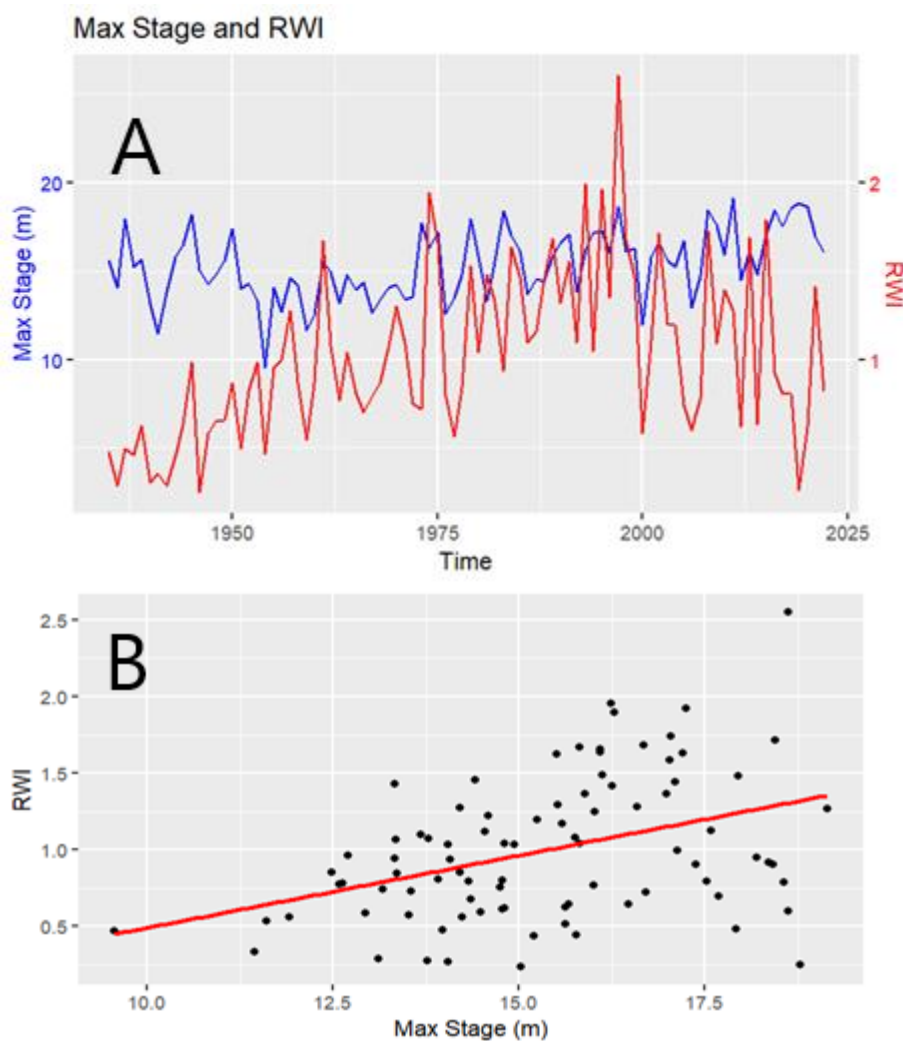


**Figure 27:** (A) Maximum stage record at Red River Landing, LA compared to RWI record. (B) Best-fit linear relationship (red line) between both records.

Every year in the Red River Landing LMR period of record has sufficient maximum stage level to inundate Cat Island NWR for some period except for the years 1941, 1954, 1959 and 2000: this further supports the conclusion that the river stage is a controlling

factor on baldcypress growth. Since duration of inundation and maximum stage are correlated, e.g., more higher stage occurrences equate with longer inundation periods (Figure 28), both factors provide a link to water availability for growth in baldcypress.

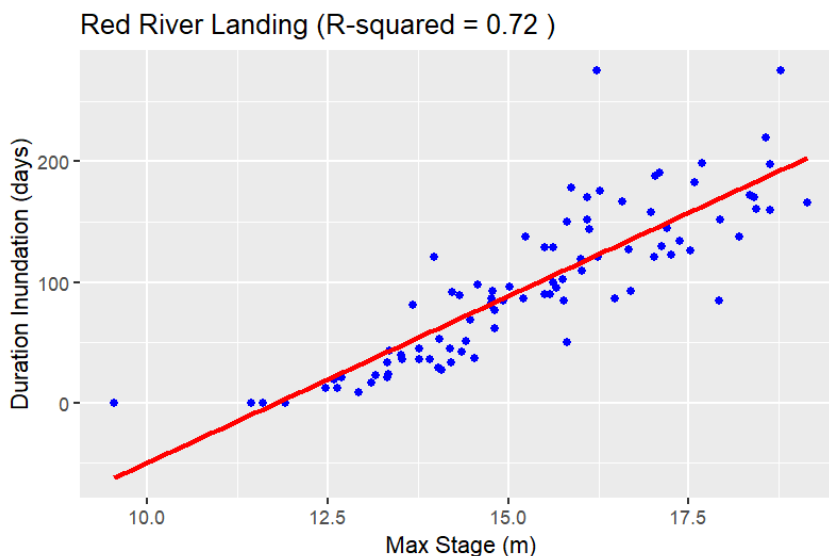


**Figure 28:** Relationship between duration of inundation in the study area and yearly maximum stage at Red River Landing, LA showing the direct linear relationship between increased duration and increased maximum stage.

There are no previous investigations that suggest an excessive depth of inundation will independently shut down baldcypress growth, and in the present study even the highest observed stages do not show a clear change in the linear relationship with RWI (Figure 27b). In years widely known to have extreme maximum stage in the period of record from these LMR stations—1927, 1973 and 2011 (when flood height was high enough to open the Morganza Spillway)—the baldcypress chronology does not show particularly low growth rates (Figure 27b). As further support for an absence in the limitation induced by higher maximum stages, record of maximum stage at Red River Landing was split equally by stage values and the years containing higher flood levels had a similar correlation to RWI as the years containing lower flood levels (0.19 versus 0.17). Finally,

the number of flood rings each year (Figure 11) mimic the mean line of growth in Figure 10, further supporting the absence of a limitation induced by higher maximum stage.

#### *6.4.3 Water Discharge*

Discharge records in other river catchments in the southeastern US have been utilized for comparison to baldcypress dendrochronology records (Therrell and Bialecki, 2015; Therrell et al., 2020; Tucker et al., 2022). Discharge records at Baton Rouge, LA and Tarbert Landing, MS were also examined in the present study for comparison to the baldcypress chronology (Table 6). At both Red River Landing/Tarbert Landing (the stage and discharge stations are only 6.5 km apart) and Baton Rouge, LA, discharge has a less robust positive linear correlation to RWI than max stage (Red River Landing  $r = 0.398$  vs  $0.353$ , Baton Rouge  $r = 0.179$  vs  $0.008$ ) or duration of inundation calculated from stage. The reason for the higher correlation with stage are likely due, in part, to the fact that stage is a daily average measurement made at sub-hourly intervals, while discharge at the Tarbert Landing and Baton Rouge USGS stations are only collected by boat measurement 10-14 times/yr and daily discharges are derived from constructing a stage:discharge ratings curve. Uncertainty in the stage:discharge ratings curve induced by hysteresis in the hydrograph (Perret et al., 2022) will serve to make river discharge a less accurate predictor of overbanking maximum level and duration into the floodplain. The stage:discharge ratings curve is also likely to shift within the period of record if there are changes in channel geometry in the station reach. Biedenharn et al. (2017) found the specific gage at Red River Landing has been rising since the 1940s which they attributed to channel bed aggradation (Figure 29). This indicates that in the reach of the LMR opposite Cat Island NWR, a given volume of water has caused a variable degree of

flooding into the floodplain over time. An additional error in utilizing water discharge as the comparative parameter with RWI, is that cross-sectional channel measurements have a significant instrument error (Edwards and Glysson, 1999). It can be concluded that water surface elevation (stage), because it is a high fidelity, high frequency measurement, is the best measure of the depth and duration of inundation into the floodplain of the LMR during overbanking periods.

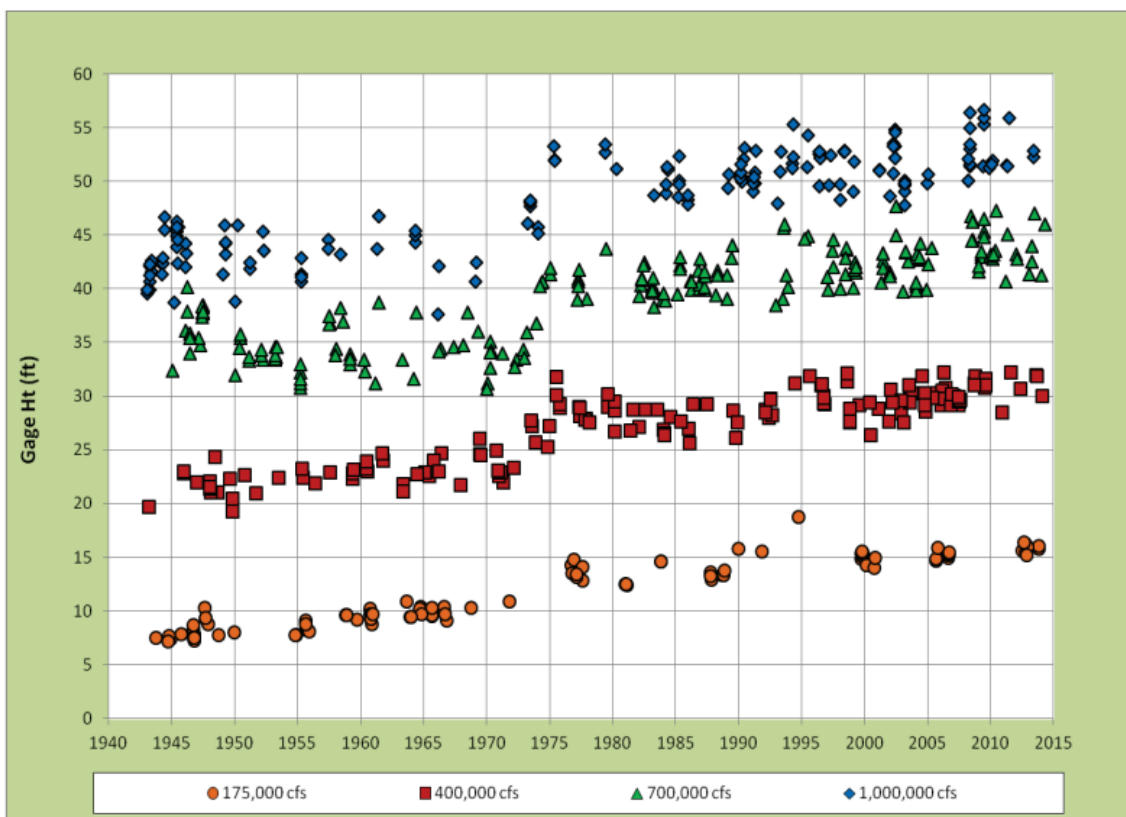


**Figure 29:** Specific gage record at Red River Landing, LA (RM 302.4) (from Biedenharn et al., 2017). Note the stepwise increase in specific gage after the large 1973 flood.

#### 6.4.4 Correlation with Seasonal Timing of Flooding

Over the period of record, maximum LMR stage has occurred in all months except August to October (Figure 16). A seasonality correlation was performed to display the relationship between month of maximum stage and baldcypress growth rates

using the long and well-linked record for hydrological parameters at Red River Landing, LA (Figure 30). The highest correlations with RWI are in June and July, the middle of the baldcypress growing season. It should be noted that the yearly maximum stage also occurs most frequently in April and May (Figure 16), and typically leaves the floodplain inundated during June and July. The increased water availability, positively impacting tree growth, also brings in increased riverine suspended sediment particles, both mineral and organic, that may provide further nutrients for growth. The fertilizing effect of increased nutrients to the trees during the growing season likely also acts to accelerate growth rates, potentially amplifying the seasonal correlation to water availability (Day et al., 2006).

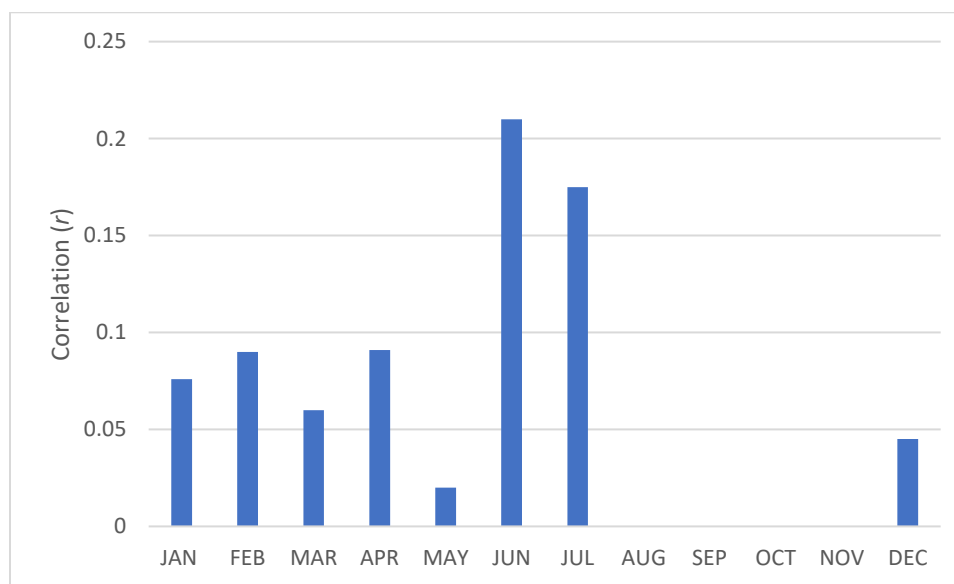


**Figure 30:** Correlation of baldcypress RWI index to month of maximum stage occurrence at Red River Landing, LA by month.

### **6.5 Relationship to MR Historic Engineering**

The geomorphology and hydrology of the LMR channel and connectivity with the adjacent floodplain have been heavily altered due to an extensive history of engineering

(Figure 31). Engineering works that have potentially impacted stage at Cat Island NWR, and hence flooding extent in the floodplain, include upriver construction of levees raising flow lines in the LMR post-1927 flood (Lewis et al., 2018), cutoffs in 1929-1942 that lowered stage by increasing downstream conveyance (Biedenharn et al., 2000) and the ORCC and Morganza releasing water. Further, stream power loss at Morganza during large flow events (e.g., 1973 and 2011) and the ORCC potentially impact sediment delivered during overbank events by reducing channel suspended sand and fines concentrations (Allison et al., 2012; Allison and Pratt, 2017). This could potentially impact particle-phase nutrient delivery to the floodplain baldcypress trees at Cat Island NWR. This disruption in water and sediment conveyance, also is thought to lead to channel bed aggradation in the reach below ORCC (including Cat Island NWR) as noted by observed specific gauge migration (Biedenharn et al. 2017). This would have tended to increase the stage of a given discharge flood. Durations of flooding at Cat Island NWR have certainly been on the rise overall since the 1950's (Figure 26), however, this has also been a period of generally rising discharge in the LMR reach (Figure 19)—making it difficult to deconvolve the engineering and hydrological drivers. Through this period of widespread engineering changes to the LMR (Figure 31), it should be emphasized that the study area has had no artificial leveeing, making the overbank elevations into the Cat Island NWR floodplain static. However, the presence of revetments has halted any potential channel migration that may impact tree age and duration of overbank flow received by the section of the floodplain. Additionally, in the absence of bankline migration, natural levee elevations may have increased due to sediment delivery more than if the channel was migrating laterally, eroding at the natural

levees and migrating the locus of sedimentation. This is supported by the high (>20 cm/yr) feldspar plot deposition rates measured at several locations on the Cat Island NWR natural levee by Myers (2022) and in the current study (Figure 21).

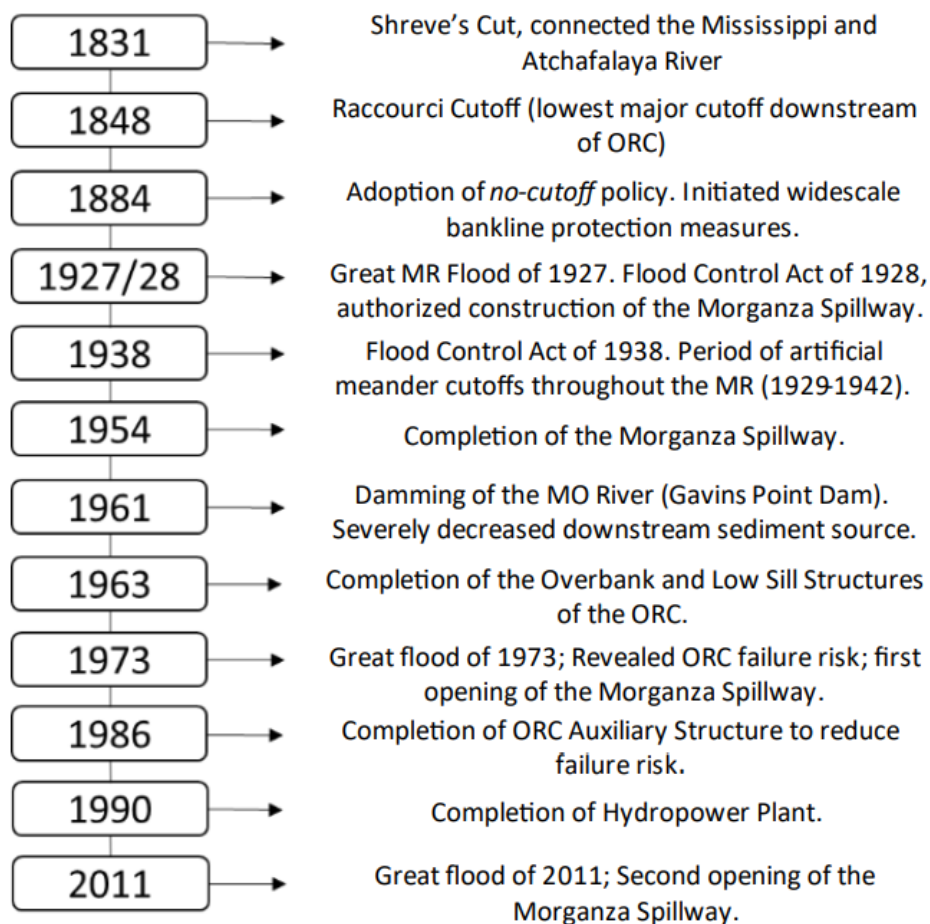


**Figure 31:** Condensed timeline of engineering on the LMR reach between ORCC and Baton Rouge (from Myers, 2022).

As mentioned above, in the LMR study reach there are increases in maximum stage (Figure 27) and duration of annual inundation (Figure 26) into Cat Island NWR utilizing the Red River Landing record since 1975 and in LMR discharge from the Tarbert Landing record since 1930 (Figure 19) suggesting a basin level change. In tandem with

the increases seen in Figures 19, 25, 26, an increase is seen in the RWI from the early 1940s until the late 1990s. This may be attributable to the completion of the cut-off program in 1942 and the rising specific gage at Red River Landing, LA (as well as increasing river discharge) since the 1940s (Figure 29, Biedenharn et al., 2017). Increases in specific gage for both high and low flows are present in the reach below ORCC opposite Cat Island NWR, particularly in the post-cutoff era (Biedenharn et al., 2017). The increase in specific gage post-1973 flood (Figure 29) occurs in tandem with increases in maximum stage (Figure 27) and duration of inundation (Figure 26), which is mirrored in a secondary increase in growth in the baldcypress chronology starting in 1975. Figure 10 displays a significant decrease in growth since the 1990s, which does not correlate with observed changes in specific gage and water discharge outlined above. While the exact causality of this RWI decrease is not apparent, it may be attributable to declining stream power and ongoing losses from the basin (Allison et al., 2012).

Further changes in the water discharge can be associated with historical trends associated with water capture in the Atchafalaya pathway. While the overall discharge of the LMR has been increasing at Tarbert Landing below ORCC (Figure 32), percentage of flow making it to the reach below ORCC has been relatively static. The RWI growth record has been increasing, not static. It can be concluded that, despite the presence of ORCC, rising discharges from the basin and increasing specific gage in the reach opposite Cat Island NWR have been the driver of increasing stage and Cat Island NWR inundation, and on RWI growth rates during the last century. It should be noted that the ORCC became operational in 1963, meaning water loss prior to this date was not attributable to local engineering. The percentage decrease from 1930 to 1975 reflects the Atchafalaya

increasing capture during this period (Roberts, 1998). After completion of the ORCC, an increase in the difference in discharge from Vicksburg to Tarbert Landing can be observed (Figure 32). This may be a function of a progressive decline in flow from the Red River, requiring more water to be taken from the LMR to maintain the 70:30 split. These local changes to the LMR may explain lower-than-anticipated correlations between LMR hydrologic records and RWI.

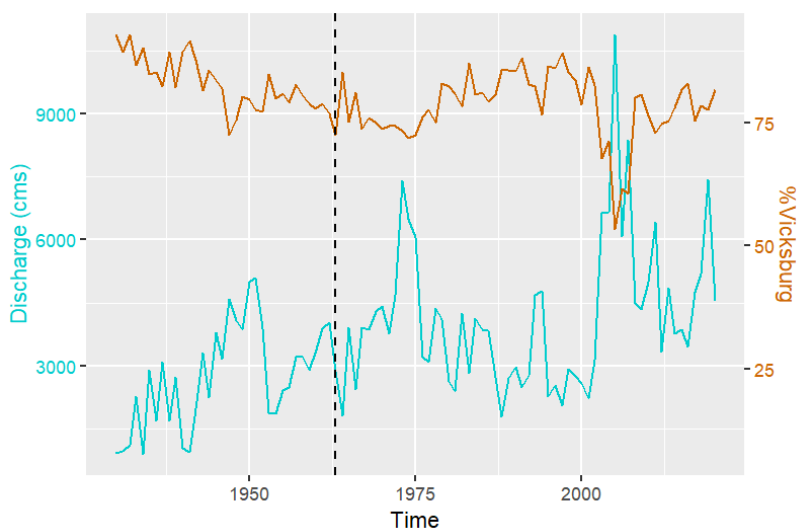


**Figure 32:** Difference in water at Vicksburg (above ORCC) and Tarbert Landing (below ORCC). This is displayed by the blue line as total difference in discharge from Vicksburg to Tarbert Landing and by the brown line as percent of Vicksburg discharge present at Tarbert Landing. The vertical line at 1963 represents the completion of the ORCC.

### 6.6 Future Considerations for Utilizing Baldcypress Chronologies

The present study indicates that there are multiple drivers of growth rates in baldcypress in the floodplain at Cat Island NWR—local elevation that impacts inundation depth and frequency during LMR overbanking events, regional climate and site level hydrology and soil characteristics (e.g., sediment input and grain size). The LMR system is a continental-scale catchment, with climate from a large geographical area affecting the

conditions at the study area reach. While the baldcypress chronology does reflect the LMR hydrological record, this correlation should be interpreted cautiously and with consideration for the other environmental drivers of tree growth outlined in this study when being used to reconstruct long-term or paleo-flood records.

There are several drivers of tree growth at Cat Island NWR that are unrelated to LMR hydrology and should be considered when examining the linkage of RWI with past flooding:

- (1) Local climatology (Table 5) is recorded to impact baldcypress growth in the present study and this link has also been recorded previously (Stahle et al., 2012; Meko and Therrell, 2020; Therrell et al., 2020; Tucker et al., 2022).
- (2) Varying amounts of sediment load and dissolved nutrients carried in the LMR and subsequently into the floodplain impacts nutrient amounts available to trees. Suspended sediment loads in the LMR have been decreasing since the 1950s (Meade and Moody, 2009; Allison and Pratt, 2017).
- (3) Elevation differences induced by the topography of the floodplain influences water availability and, hence, impacts tree growth.
- (4) Site biotic factors such as competition light and nutrients impact the growth rates of individual trees.
- (5) Soil types vary across the floodplain generally controlled by distance from the river channel—sediment grain size overall decreases from the natural levee to the backswamp.

It should be emphasized that further complexity of correlating the baldcypress chronology to the LMR hydrologic record is due to the enormous basin size of the Mississippi River and that, while no singular correlation to growth drivers is particularly strong, the correlations to the LMR hydrology (stage and discharge) are the highest. Future studies and usage of baldcypress chronologies to correlate to or reconstruct historical river hydrology may be more effective in smaller river basins. The present study site was advantageous as it is contained within an area that receives the same hydrologic regime giving hydrologic stability and is of small elevation range. These study area conditions are recommended for future baldcypress studies. However, to improve the utility of baldcypress chronologic reconstruction of LMR hydrology, future studies could benefit from obtaining additional, widely separated (100's of km apart) sites to establish a "master basin chronology" where RWI trend similarities with the record at Cat Island NWR could be examined to help distinguish between hydrological factors from the non-hydrological controls outlined in 1-5 above.

## 7. CONCLUSIONS

The results of the present study of Cat Island NWR floodplain lead to the following conclusions:

(1) Baldcypress trees in Cat Island NWR contain a dendrochronological record of annual flood magnitude and duration that can potentially document anthropogenic hydrological changes wrought by human engineering of the LMR.

(2) Relating the interannual baldcypress growth record (RWI) to hydrological factors like LMR stage is complicated by other factors that impact growth rates in the study area including local climatology, basin-wide climatology, varying sediment loads, tree elevation, biotic factors and soil type. The correlation to the LMR historical stage record is the highest amongst all tested factors in this study, but these additional factors help to explain why the relationship is not better correlated despite the indications that growth rates are positively correlated to flooding duration and magnitude in the Cat Island NWR floodplain. The study does indicate that longer tree cores that go further back in time at Cat Island NWR and elsewhere in the LMR basin have the potential to provide insights into historical stage prior to the onset of river monitoring in the latter half of the 19<sup>th</sup> century.

(3) Using tree ring records to examine changes in growth related to changes in the hydrology of adjacent rivers can give insight into the impacts that changes to the channel will make on the floodplain and should be considered in future management decisions. This can be monitored through growth patterns. Baldcypress at Cat Island NWR is often

a stand-level dominant tree, many being older than 100 years, making the species a satisfactory monitor of changes in forest health over time.

## APPENDICES

*Appendix A: Baldecypress Chronology Information**Table A1: Years in each tree ring series containing false rings. Blue column denotes number of years per tree.*

TADIO01	TADIO04	TADIO8A	TADIO8B	TADI12A	TADI12B	TADI16A	TADI16B	TADI17A	TADI17B	TADI21A	TADI21B	TADI25B
20	54	14	11	43	56	23	30	36	37	23	36	47
1987	2018	1996	1987	2013	2013	2001	2004	2013	1995	1998	2010	2010
1986	2015	1993	1973	2003	2003	1998	1999	10	1990	1995	2009	2009
1985	2012	1992	1969	2001	2001	1982	1996	2010	1989	1993	2007	2008
1984	2011	1990	1961	1998	1999	1969	1995	2004	1988	1992	2004	2006
1983	1987	1989	1928	1988	1998	1968	1988	1993	1984	1991	2003	2003
1982	1970	1964	1925	1987	1994	1957	1987	1992	1979	1990	2002	2002
1981	1966	1961	1924	1986	1993	1956	1986	1990	1975	1989	2001	1999
1978	1964	1960	1922	1985	1991	1955	1985	1988	1974	1988	1999	1999
1977	1961	1957	1921	1984	1990	1928	1983	1983	1971	1982	1998	1998
1976	1957	1945	1918	1983	1989	1924	1982	1982	1970	1981	1997	1997
1975	1956	1928	1912	1982	1988	1919	1980	1981	1969	1969	1996	1996
1974	1955	1926		1981	1987	1917	1979	1979	1964	1967	1995	1995
1973	1952	1925		1980	1986	1909	1977	1975	1963	1966	1994	1994
1972	1951	1922		1979	1984	1908	1968	1970	1962	1963	1993	1993
1971	1949			1977	1983	1905	1963	1962	1961	1962	1992	1992
1970	1947			1975	1982	1904	1957	1961	1956	1961	1991	1991
1969	1939			1974	1981	1902	1953	1958	1952	1960	1990	1989
1967	1938			1972	1980	1898	1952	1955	1951	1959	1989	1988
1961	1937			1971	1979	1895	1948	1953	1950	1958	1988	1987
1958	1937			1970	1978	1892	1934	1943	1945	1956	1987	1986
	1936			1969	1977	1887	1928	1940	1938	1955	1986	1985
	1935			1968	1976	1884	1919	1939	1936	1951	1984	1984
	1934			1967	1975	1871	1915	1933	1935	1949	1983	1983
	1933			1965	1974		1902	1932	1934		1982	1982
	1929			1964	1972		1896	1918	1921		1981	1980
	1928			1962	1971		1890	1911	1920		1979	1979
	1927			1961	1970		1865	1905	1916		1978	1975
	1924			1960	1969		1864	1902	1913		1977	1974
	1923			1957	1967		1857	1900	1912		1976	1973
	1917			1956	1965		1856	1896	1907		1975	1972
	1914			1954	1963			1895	1906		1974	1969
	1913			1950	1962			1894	1892		1973	1968
	1912			1948	1961			1890	1889		1972	1967
	1911			1947	1960			1889	1886		1971	1966
	1910			1945	1958			1888	1885		1970	1965
	1908			1943	1957			1885	1882		1968	1964
	1907			1939	1956				1881			1963
	1906			1934	1955							1962
	1905			1924	1950							1961
	1904			1922	1949							1958
	1903			1921	1947							1957
	1902			1920	1945							1956
	1901			1918	1939							1955
	1900				1938							1953
	1896				1937							1952
	1895				1934							1950
	1894				1933							1945
	1892				1930							
	1890				1929							
	1889				1927							
	1888				1925							
	1887				1924							
	1886				1922							
	1885				1917							
					1901							
					1896							

TADI26A	TADI27A	TADI27B	TADI29A	TADI29B	TADI30A	TADI30B	TADI38B	TADI40A	TADI40B
30	31	52	33	40	31	25	23	26	24
2017	2010	2015	2010	2015	2001	2004	2010	2021	2021
2010	2001	2003	2003	2010	1998	2001	2009	2017	2017
2009	1996	2002	2001	2009	1996	1998	2008	2013	1997
1998	1995	1996	1999	2007	1989	1993	2007	1999	1995
1997	1994	1995	1996	2003	1986	1992	1997	1998	1994
1996	1993	1994	1995	1999	1985	1991	1994	1997	1991
1995	1991	1993	1993	1998	1984	1989	1993	1995	1990
1993	1989	1987	1992	1996	1983	1986	1990	1993	1989
1992	1987	1986	1991	1994	1980	1985	1989	1991	1988
1990	1986	1985	1990	1993	1979	1984	1988	1990	1985
1989	1985	1984	1989	1992	1975	1983	1986	1989	1982
1988	1981	1981	1988	1991	1974	1982	1985	1988	1981
1987	1974	1975	1987	1990	1968	1981	1984	1986	1977
1984	1972	1974	1986	1989	1966	1978	1980	1985	1975
1983	1964	1973	1985	1988	1964	1977	1979	1984	1974
1981	1963	1970	1982	1987	1928	1976	1978	1982	1973
1979	1957	1966	1980	1986	1919	1975	1977	1975	1966
1978	1956	1964	1978	1985	1912	1971	1976	1974	1965
1975	1950	1961	1977	1982	1897	1968	1975	1973	1952
1974	1949	1956	1976	1981	1894	1961	1971	1970	1949
1970	1948	1955	1974	1980	1890	1938	1970	1967	1947
1969	1939	1951	1973	1977	1880	1925	1969	1966	1941
1968	1934	1949	1971	1976	1871	1920	1967	1961	1938
1961	1925	1946	1970	1975	1868	1897		1953	1937
1956	1922	1941	1969	1974	1865	1896		1952	
1954	1915	1939	1968	1973	1864			1948	
1950	1878	1930	1966	1972	1855				
1938	1877	1928	1965	1971	1854				
1925	1875	1923	1963	1969	1853				
1923	1874	1921	1960	1968	1852				
	1873	1917	1958	1966	1850				
		1916	1956	1965					
		1898	1953	1964					
		1895		1963					
		1894		1960					
		1883		1959					
		1880		1957					
		1877		1956					
		1876		1954					
		1875		1953					
		1874							
		1873							
		1872							
		1871							
		1870							
		1869							
		1868							
		1867							
		1866							
		1865							

*Table A2: Individual tree cores information including if cores are included in the final chronology, denoted by an “X”.*

<b>Sample ID</b>	<b>Chronology</b>	<b>Elevation (m)</b>	<b>DBH (m)</b>
TADI0001	X	8.8	
TADI0004	X	9.8	
TADI0005		9.8	
TADI0006		9.8	
TADI0007		13.7	
TADI08A	X	13.7	
TADI08B	X	13.7	
TADI09A		11.6	
TADI09B		11.6	
TADI10A		10.4	
TADI10B		10.4	
TADI11A		10.7	
TADI11B		10.7	
TADI12A	X	10.7	
TADI12B	X	10.7	
TADI13A		10.4	0.64
TADI13B		10.4	0.89
TADI14A		10.4	0.56
TADI14B		10.4	0.56
TADI15A		10.4	0.49
TADI15B		10.4	0.49
TADI16A	X	10.4	0.61
TADI16B	X	10.4	0.61
TADI17A	X	10.4	0.52
TADI17B	X	10.4	0.52
TADI18A		10.4	0.53
TADI18B		10.4	0.53
TADI19A		10.1	1.01
TADI19B		10.1	1.01
TADI20A		10.4	0.56
TADI20B		10.4	0.56
TADI21A		10.4	0.77
TADI21B		10.4	0.77
TADI22A		10.1	1.83
TADI22B		10.1	1.83
TADI23A		10.7	1.12
TADI23B		10.7	1.12
TADI24A		11.3	0.52
TADI24B		11.3	0.52
TADI25A		10.7	0.26

TADI25B	X	10.7	0.26
TADI26A	X	10.7	0.55
TADI26B		10.7	0.55
TADI27A	X	11.0	0.64
TADI27B	X	11.0	0.64
TADI28A		10.7	0.64
TADI28B		10.7	0.64
TADI29A	X	10.1	0.74
TADI29B	X	10.1	0.74
TADI30A	X	10.7	0.72
TADI30B	X	10.7	0.72
TADI31A		9.1	1.00
TADI31B		9.1	1.00
TADI32A		9.4	0.73
TADI32B		9.4	0.73
TADI33A		9.4	0.41
TADI33B		9.4	0.41
TADI34A		11.0	0.70
TADI34B		11.0	0.70
TADI35A		10.1	
TADI35B		10.1	
TADI36A		11.6	0.64
TADI36B		11.6	0.64
TADI37A		13.7	0.56
TADI37B		13.7	0.56
TADI38A		11.6	0.37
TADI38B	X	11.6	0.37
TADI39A		12.5	0.44
TADI39B		12.5	0.44
TADI40A	X	13.4	0.51
TADI40B	X	13.4	0.51
TADI41A		14.0	0.49
TADI41B		14.0	0.49
TADI42A		13.4	0.46
TADI42B		13.4	0.46
TADI43A		13.7	0.48
TADI43B		13.7	0.48
TADI44A		13.4	0.46
TADI44B		13.4	0.46

**Appendix B: Deposition field measurements**

**Table B1:** Feldspar plot sediment measurements for WY 2023. Includes sediment from WY 2021 and 2022 except for new plots. \*Denotes plot initiated in WY 2022 and includes deposition for WY 2023 and 2022. \*\*Denotes that the plot was not found in WY 2022, therefore only a combined measurement can be made for WY 2022 and 2023.

Site #	Deposition (mm)
19	13
20	16
21	28
22	22
23**	20
24	NA
27	9
28	22
29	140
30	750
34	24
35	33
36	22
37	25.5
50*	11
51*	20

**Table B2:** Feldspar plot sediment measurements for WY 2022. Includes sediment from WY 2021 except for new plots. \*Denotes new plots for WY 2022

Site #	Deposition (mm)
1	190
2	35
3	19
4	10
5	6
6	35
27	7.5
28	14
29	80
30	625
34	15
36	13
37	17
38	21
39	6
50*	6
51*	11
52*	2
53*	1.5

**Table B3:** Feldspar plot sediment measurements for WY 2021 (Myers, 2022).

Site #	Deposition (mm)
1	230
2	10
3	22
4	15
5	4.5
6	37
7	70
9	25
11	25
14	35
15	45
16	32.5
17	75
18	NA
19	6
20	4
21	NA
22	12
23	13
24	NA
27	1.5
28	10
28.5	20
29	34.5
30	290
31	6
32	14.25
33	24
34	16.5
35	9
36	12
37	12.5
38	5.5
39	11.5
40	6.5
41	9

**Table B4:** Sediment deposition measured from  $^7\text{Be}$  activity for WY 2020 (Myers, 2022).

Site #	Deposition (mm)
1	27.5
2	12.5
3	17.5
4	22.5
5	17.5
6	27.5
7	11.5
8	12.5
9	27.5
10	22.5
11	17.5
12	27.5
18	15
32	15
34	17.5
38	17.5
41	17.5

**Appendix C: Individual Baldcypress Correlations**

**Figure C1:** Relationship between duration of inundation from HOB0 water level logger 34 and RWI of TADI01.

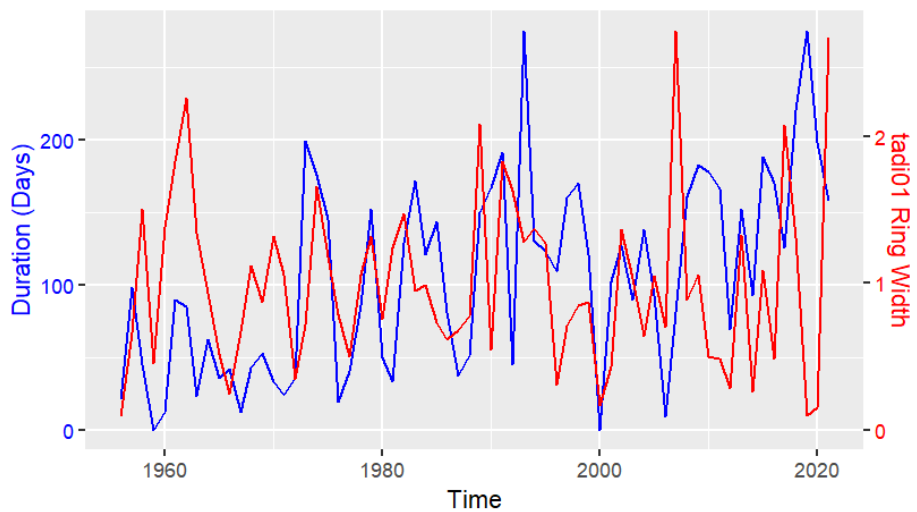


**Figure C2:** Relationship between duration of inundation from HOB0 water level logger 53 and RWI of TADI12. TADI12 includes TADI12A and TADI12B.

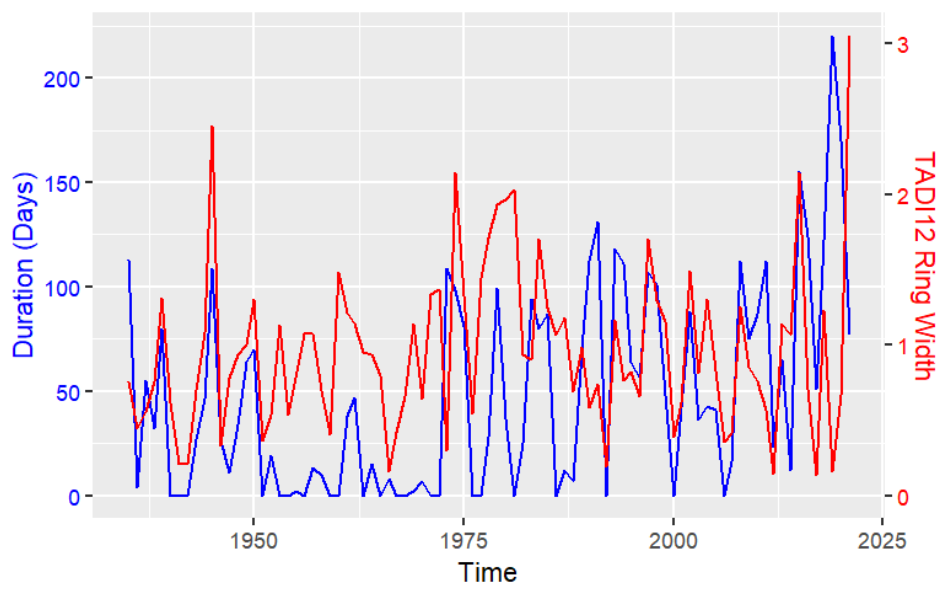
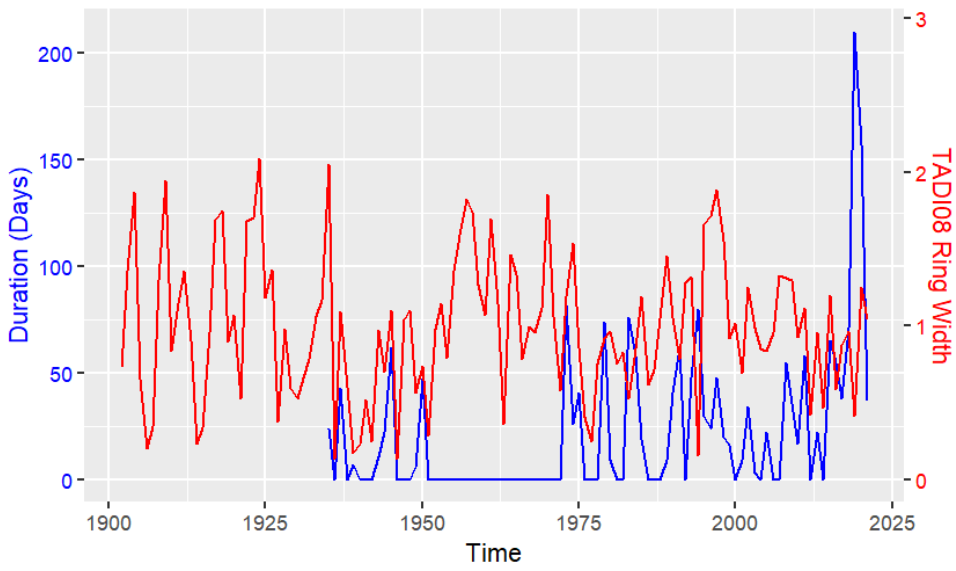


**Figure C3:** Relationship between duration of inundation from HOB0 water level logger 50 and RWI of TADI08. TADI08 includes TADI08A and TADI08B.



## 8. REFERENCES

- Alexander, J.S., Wilson, R.C., and Green, W.R., 2012. A Brief History and Summary of the Effects of River Engineering and Dams on the Mississippi River System and Delta. US Geological Survey Circular 1375
- Allison, M.A., Demas, C.R., Ebersole, B.A., Kleiss, B.A., Little, C.D., Meselhe, E.A., Powell, N.J., Pratt, T.C., and Vosburg, B.M., 2012. A water and sediment budget for the lower Mississippi-Atchafalaya River in flood years 2008-2010: Implications for sediment discharge to the oceans and coastal restoration in Louisiana. *J. Hydrol.*, 432, 84-97. DOI: 10.1016/j.jhydrol.2012.02.020.
- Allison, M.A. and Pratt, T.C., 2017. Discharge controls on the sediment and dissolved nutrient transport flux of the lowermost Mississippi River: Implications for export to the ocean and for delta restoration. *Journal of Hydrology.*, 555, 1-14. DOI: <https://doi.org/10.1016/j.jhydrol.2017.10.002>
- Atlas: The Louisiana Statewide GIS. LSU CADGIS Research Laboratory, Baton Rouge, LA, 2009. <http://atlas.lsu.edu>
- Biedenharn, D.S., Allison, M.A., Little, C.D., Thorne, C.R., and Watson, C.C. 2017. Large-scale geomorphic change in the Mississippi River from St. Louis, MO, to Donaldsonville, LA, as revealed by specific gage records. MRG&P Technical Report No. 10. <https://hdl.handle.net/11681/22744>
- Biedenharn, D.S., Killgore, K.S., Little, C.D. Jr., Murphy, C.E., and Kleiss, B.A. 2018. Attributes of the Lower Mississippi River Bature. MRG&P Technical Note No. 4.
- Biedenharn, D.S., Thorne, C.R., and Watson, C.C. 2000. Recent morphological evolution of the Lower Mississippi River. *Geomorphology.*, 34, 227-249.
- Bunn, A., Korpela, M., Biondi, F., Campelo, F., Mérian, P., Qeadan, F., and Zang, C. 2022. dplR: Dendrochronology Program Library in R. R package version 1.7.3. <https://CRAN.R-project.org/package=dplR>
- Day, R. H., Doyle, T. W., & Draugelis-Dale, R. O. 2006. Interactive effects of substrate, hydroperiod, and nutrients on seedling growth of *Salix nigra* and *Taxodium distichum*. *Environmental and Experimental Botany*, 55(1), 163-174. <https://doi.org/https://doi.org/10.1016/j.envexpbot.2004.10.009>
- Deshpande, A., Boutton, T., Hyodo, A., Lafon, C., & Moore, G. 2020. Bottomland hardwood forest growth and stress response to hydroclimatic variation: evidence from dendrochronology and tree ring  $\Delta^{13}\text{C}$  values. *Biogeosciences*, 17, 5639-5653. <https://doi.org/10.5194/bg-17-5639-2020>
- Eggler, W.A. 1955. Radial growth in nine species of trees in southern Louisiana. *Ecology*, 36(1): 130–136. doi:10.2307/1931438.

- Harris, I., Osborn, T.J., Jones, P. et al. 2020. Version 4 of the CRU TS monthly high-resolution gridded multivariate climate dataset. *Sci Data* 7, 109. <https://doi.org/10.1038/s41597-020-0453-3>
- Holmes, R.L. 1983. Computer-assisted quality control in tree-ring dating and measurement. *Tree-Ring Bulletin* 43: 69-78. Holmes, R.L. 1983. Computer-assisted quality control in tree-ring dating and measurement. *Tree-Ring Bulletin* 43: 69-78.
- Frank, D., Fang, K., & Fonti, P. 2022. Dendrochronology: Fundamentals and Innovations. In R. T. W. Siegwolf, J. R. Brooks, J. Roden, & M. Saurer (Eds.), *Stable Isotopes in Tree Rings: Inferring Physiological, Climatic and Environmental Responses* (pp. 21-59). Springer International Publishing. [https://doi.org/10.1007/978-3-030-92698-4\\_2](https://doi.org/10.1007/978-3-030-92698-4_2)
- Gulliver, J.S., Erickson, A.J., and Weiss, P.T. 2010. *Stormwater Treatment: Assessment and Maintenance*. University of Minnesota, St. Anthony Falls Laboratory. Minneapolis, MN. <https://stormwaterbook.safl.umn.edu/>
- Edwards, T. K., and Glysson, G.D. 1999. Field methods for measurement of fluvial sediment, in *Techniques of Water-Resources Investigation of the U. S. Geological Survey, Book 3*, 97 pp., U.S. Geol. Surv., Reston, VA.
- Keeland, B.D. and Conner W.H. 1999. Natural regeneration and growth of *Taxodium distichum* (L.) Rich. in Lake Chicot Louisiana after 44 years of flooding. *Wetlands* 19: 149–155.
- Keim, R., and Amos, J. 2012. Dendrochronological analysis of baldcypress (*Taxodium distichum*) responses to climate and contrasting flood regimes. *Canadian Journal of Forest Research*, 42, 423-436. <https://doi.org/10.1139/x2012-001>
- Kleiss, B.A. 1996. Sediment Retention in a Bottomland Hardwood Wetland in Eastern Arkansas. *Wetlands*, 16-3, 321-333.
- Lewis, J., McKinnie, C., Parrish, K., Crosby, W., Cruz, C., Dove, M., Gaines, R.A., Gambill, R., Ramirez, D., Taylor, R., Agnew, M., Veatch, W., Dirksen, M., Brown T., Griggs, F., Copeland, R., Rentfro, B., Ashley, J., Windham, J., and Howe, E. 2018. Mississippi River and Tributaries Flowline Assessment Main Report. In: *Mississippi River Geomorphology and Potamology Program (MRG&P) Report No. 24-1*, December 2018. USACE, Mississippi Valley Division: Vicksburg, MS.
- Li, X., Tian, H., Pan, S., and Lu, C. 2022. Four-century history of land transformation by humans in the United States: 1630-2020. *Earth System Science Data*. <https://doi.org/10.5194/essd-2022-135>

- Magliolo, C.R. 2017. Overbank Deposition of Sand and Mud within Two Point Bars Bound by the Mississippi River Levee System: Implications for Coastal Restoration Sediment Budgets. LSU Master's Theses. 4326. [https://digitalcommons.lsu.edu/gradschool\\_theses/4326](https://digitalcommons.lsu.edu/gradschool_theses/4326)
- Meade, R.H. and Moody, J.A. 2009. Causes for the decline of suspended-sediment discharge in the Mississippi River system, 1940-2007. *Hydrol. Process.* 24, 35-49. DOI: 10.1002/hyp.7477
- Meitzen, K. M. 2018. Floodplains. In Reference Module in Earth Systems and Environmental Sciences. Elsevier. <https://doi.org/https://doi.org/10.1016/B978-0-12-409548-9.11027-9>
- Moore, N.R. 1972. Improvements of the Lower Mississippi River and tributaries, 1937-1972. US Army Corps of Engineers Mississippi River Commission: Vicksburg, MS.
- Murray, A. S., and Biedenbarn, D. S. 2022. (rep.). Sediment Supply from Bank Caving on the Lower Mississippi River, 1765 to Present. Engineer Research and Development Center: Vicksburg, MS. Retrieved February 4, 2023, from <https://apps.dtic.mil/sti/citations/AD1179714>.
- Myers, R. 2022. Floodplain sedimentation in the lowermost Mississippi River (Unpublished master's thesis). Tulane University, New Orleans, Louisiana.
- Roberts, H. H. 1998. Delta Switching: Early Responses to the Atchafalaya River Diversion. *Journal of Coastal Research*, 14(3), 882-899. <https://www.jstor.org/stable/4298842>
- Smith, M. and Bentley, S.J. 2014. Sediment capture in flood plains of the Mississippi River: A case study in Cat Island National Wildlife Refuge, Louisiana. *Sediment Dynamics from the Summit to the Sea*. IAHS Publication 367.
- Systematic Remote Sensing and Computer Cartography Laboratory (SRCC), Texas A&M University. 2023. SRCC - Texas A&M University. <https://www.srcc.tamu.edu/>
- Speer, J. H. 2010. *Fundamentals of tree-ring research*. University of Arizona Press.
- Stahle, D. W., Burnette, D. J., Villanueva, J., Cerano, J., Fye, F. K., Griffin, R. D., Cleaveland, M. K., Stahle, D. K., Edmondson, J. R., & Wolff, K. P. 2012. Tree-ring analysis of ancient baldcypress trees and subfossil wood. *Quaternary Science Reviews*, 34, 1-15. <https://doi.org/https://doi.org/10.1016/j.quascirev.2011.11.005>
- Stoffel, M., Bollschweiler, M., 2008. Tree-ring analysis in natural hazards research – an overview. *Nat. Hazard. Earth Syst. Sci.* 8, 187–202.

- Therrell, M. D., & Bialecki, M. B. 2015. A multi-century tree-ring record of spring flooding on the Mississippi River. *Journal of Hydrology*, 529, 490-498. <https://doi.org/https://doi.org/10.1016/j.jhydrol.2014.11.005>
- Therrell, M., Elliott, E., Meko, D., Bregy, J., Tucker, C., Harley, G., Maxwell, J., & Tootle, G. 2020. Streamflow Variability Indicated by False Rings in Baldcypress (*Taxodium distichum* (L.) Rich.). *Forests*. <https://doi.org/10.3390/f11101100>
- Tucker, C. S., Pearl, J. K., Elliott, E. A., Bregy, J. C., Friedman, J. M., & Therrell, M. D. 2022. Baldcypress false ring formation linked to summer hydroclimatic extremes in the southeastern United States. *Environmental Research Letters*. <http://iopscience.iop.org/article/10.1088/1748-9326/ac9745>
- Mississippi River Commission. 2007. The Mississippi River & Tributaries Project: History of the Lower Mississippi River Levee System. Information Paper
- Pinter, N., Jemberie, A. A., Remo, J. W. F., Heine, R. A., and Ickes, B. S. 2008, Flood trends and river engineering on the Mississippi River system, *Geophys. Res. Lett.*, 35, L23404, doi:10.1029/2008GL035987.
- Regent Inc. (2001) WinDendro Tree Ring Increment Measurement Software and XL Stem 1.3 Macro.
- USDA, NRCS. 2024. The PLANTS Database (<http://plants.usda.gov>, 01/31/2024). National Plant Data Team, Greensboro, NC USA.
- USACE (U.S. Army Corps of Engineers). 2019. Lower Mississippi River floodplain landcover. GIS file produced by Mapping Science Laboratory, Texas A&M University.
- USACE (U.S. Army Corps of Engineers). 2023. Public Notice: Tunica Swamps-Silos Mitigation Area – Amendment One in West Feliciana Parish. USACE, New Orleans District. [https://www.mvn.usace.army.mil/Portals/56/docs/regulatory/publicnotices/2021\\_00058\\_PNall.pdf](https://www.mvn.usace.army.mil/Portals/56/docs/regulatory/publicnotices/2021_00058_PNall.pdf)
- USGS Surface-Water Daily Data for the Nation. Retrieved November 30, 2022, from <https://waterdata.usgs.gov/nwis/dv?>
- US Department of Commerce, N. O. A. A. 2019. *Mississippi River flood history 1543-present*. National Weather Service. Retrieved January 31, 2023, from [https://www.weather.gov/lix/ms\\_flood\\_history](https://www.weather.gov/lix/ms_flood_history)
- Weeks, L. 2016. Old River Control Structure. [https://www.johnweeks.com/river\\_mississippi/pages/lmiss23.html](https://www.johnweeks.com/river_mississippi/pages/lmiss23.html). Accessed. November 16, 2022.

- Wilhite, L. E and J. R. Toliver. 1990. *Taxodium distichum* (L.) Rich. Baldcypress. p. 563-572. In R. M. Burns and B. H. Honkala (tech. coords.) *Silvics of North America, Volume I, Conifers*. United States Department of Agriculture, Forest Service, Washington, DC, USA. Agriculture Handbook 654.
- Xu, K., Wang, X., Liang, P., An, H., Sun, H., Han, W., & Li, Q. (2017). Tree-ring widths are good proxies of annual variation in forest productivity in temperate forests. *Scientific Reports*, 7(1), 1945. <https://doi.org/10.1038/s41598-017-02022-6>
- van der Schrier, G., Barichivich, J., Briffa, K.R., and Jones, P.D. 2013. A scPDSI-based global data set of dry and wet spells for 1901-2009. *J. Geophys. Res. Atmos.* 118, 4025-4048 [10.1002/jgrd.50355](https://doi.org/10.1002/jgrd.50355).
- Yamaguchi, D. K., (1991). A simple method for cross-dating increment cores from living trees. *Canadian Journal of Forest Research*, 21(3):414-416. doi: 10.1139/X91-053

**Biography**

Kristina Leggas was born and raised in Lexington, Kentucky. After moving to Louisiana in 2017 and graduating with a B.S. in Earth and Environmental Sciences from Tulane University in 2021, she became interested in the local environment. Her fascination with local hydrology and river-coastal studies led her to pursue her master's at Tulane in Earth and Environmental Sciences.